A Section 508–conformant HTML version of this article is available at https://doi.org/10.1289/EHP11076.

Mechanisms and Consequences of Variable TRPA1 Expression by Airway Epithelial Cells: Effects of *TRPV1* Genotype and Environmental Agonists on Cellular Responses to Pollutants *in Vitro* and Asthma

Emmanuel Rapp,[1] Zhenyu Lu,[1] Lili Sun,[1] Samantha N. Serna,[1] Marysol Almestica-Roberts,[1] Katherine L. Burrell,[1] Nam D. Nguyen,[1] Cassandra E. Deering-Rice,[1] and Christopher A. Reilly[1]

[1]Department of Pharmacology and Toxicology, Center for Human Toxicology, University of Utah, Salt Lake City, Utah, USA

Background: Transient receptor potential ankyrin-1 [transient receptor potential cation channel subfamily A member 1 (TRPA1)] and vanilloid-1 [transient receptor potential cation channel subfamily V member 1 (TRPV1)] detect inhaled irritants, including air pollutants and have roles in the development and exacerbation of asthma.

Objectives: This study tested the hypothesis that increased expression of TRPA1, stemming from expression of the loss-of-function *TRPV1* (I585V; rs8065080) polymorphic variant by airway epithelial cells may explain prior observations of worse asthma symptom control among children with the *TRPV1* I585I/V genotype, by virtue of sensitizing epithelial cells to particulate materials and other TRPA1 agonists.

Methods: TRP agonists, antagonists, small interfering RNA (siRNA), a nuclear factor kappa light chain enhancer of activated B cells (NF-κB) pathway inhibitor, and kinase activators and inhibitors were used to modulate TRPA1 and TRPV1 expression and function. Treatment of genotyped airway epithelial cells with particulate materials and analysis of asthma control data were used to assess consequences of *TRPV1* genotype and variable TRPA1 expression on cellular responses *in vitro* and asthma symptom control among children as a function of voluntarily reported tobacco smoke exposure.

Results: A relationship between higher TRPA1 expression and function and lower TRPV1 expression and function was revealed. Findings of this study pointed to a mechanism whereby NF-κB promoted TRPA1 expression, whereas NF-κB–regulated nucleotide-binding oligomerization domain, leucine rich repeat and pyrin domain containing 2 (NLRP2) limited expression. Roles for protein kinase C and p38 mitogen activated protein kinase were also demonstrated. Finally, the *TRPV1* I585I/V genotype was associated with increased TRPA1 expression by primary airway epithelial cells and amplified responses to selected air pollution particles *in vitro*. However, the *TRPV1* I585I/V genotype was not associated with worse asthma symptom control among children exposed to tobacco smoke, whereas other *TRPA1* and *TRPV1* variants were.

Discussion: This study provides insights on how airway epithelial cells regulate TRPA1 expression, how TRPV1 genetics can affect TRPA1 expression, and that *TRPA1* and *TRPV1* polymorphisms differentially affect asthma symptom control. https://doi.org/10.1289/EHP11076

Introduction

Transient receptor potential ankyrin-1 [transient receptor potential cation channel subfamily A member 1 (TRPA1)] and vanilloid-1 [transient receptor potential cation channel subfamily V member 1 (TRPV1)] are cation-permeable (primarily calcium) channels involved in sensory physiology and pain.[1,2] These receptors are also proximal sensors of selected inhaled chemicals and particulate materials (PMs), and coordinate responses of lung cells exposed to environmental irritants and pneumotoxins.[3–6]

Asthma is a chronic airway inflammatory disease that is affected by exposure to environmental irritants and pollutants, including volatile/semivolatile chemicals and PM released during the combustion of various materials (e.g., petroleum products/fuels, coal, biomass/biomass-based materials, cigarettes/E-cigarettes).[7–13] TRPA1 and TRPV1 are important in the pathogenesis and exacerbation of asthma,[1,2,14–17] and the expression and activity of TRPA1[18] and TRPV1[19,20] can be elevated in the airways of people with asthma and chronic cough. Studies in mice have demonstrated a need for TRPA1 in the development of Th2-high allergic asthma phenotypes,[21] with similar findings reported for TRPV1.[22,23] Several representative PMs, including diesel exhaust particles (DEP),[4,5] wood smoke particles (WSPM),[6,24,25] and coal fly ash (CFA),[3,15,26] activate TRPA1 and TRPV1. Moreover, in airway epithelial cells (AECs), TRP activation by PM can trigger proinflammatory responses and pathological endoplasmic reticulum stress, leading to cell death. In addition, TRPA1 activation by WSPM can promote mucin 5AC (MUC5AC) expression and secretion by AECs, which could contribute to asthma exacerbation and symptomatology.[24]

Previous studies by our group demonstrated that the predominantly co-inherited *TRPA1* gain-of-function polymorphisms R3C and R58T (rs13268757 and rs16937976) correlated with reduced likelihood (relative risk = 0.27; $p = 0.14$) of achieving optimal asthma symptom control in children.[26] Studies have also shown the TRPV1 I585V (rs8065080) variant to be less responsive to canonical TRPV1 agonists and stimuli[27] and to be associated with reduced cough in people with asthma.[27,28] However, our research has shown that the *TRPV1* I585I/V genotype occurs at a higher frequency in children with moderate-to-severe steroid-resistant asthma, specifically correlating with more frequent asthma symptoms (e.g., cough/wheeze, nighttime awakenings, inhaler use, care needs; odds ratio = 2.04; $p = 0.03$) and decreased overall asthma control when compared with those with either the I585I/I or I585V/V genotypes or combinations of two additional common *TRPV1* polymorphisms (i.e., I315M; rs222747 and T469I; rs224534).[15] A basis for this clinical association was hypothesized to result from higher TRPA1 expression by AECs of individuals with the I585I/V genotype, potentially increasing the sensitivity of such individuals to common asthma triggers that activate TRPA1.

Currently, neither how TRPA1 expression is regulated by AECs, nor the basis for how the *TRPV1* I585I/V genotype promotes TRPA1 expression are understood. Moreover, the potential impact of elevated TRPA1 expression on asthma is not fully

Address correspondence to Christopher A. Reilly, Department of Pharmacology and Toxicology, Center for Human Toxicology, University of Utah, 30 S. 2000 E., Room 201 Skaggs Hall, Salt Lake City, UT 84112 USA. Telephone: (801) 581-5236. Email: Chris.Reilly@pharm.utah.edu

Supplemental Material is available online (https://doi.org/10.1289/EHP11076).

The authors declare they have nothing to disclose.

Received 8 February 2022; Revised 20 January 2023; Accepted 20 January 2023; Published 27 February 2023.

understood. Goals of this work were to *a*) understand how TRPA1 expression is regulated and specifically promoted by the *TRPV1* I585I/V genotype in AECs, *b*) determine the importance of elevated TRPA1 expression in regulating responses of AECs to pneumotoxic PM treatment, and *c*) evaluate the contribution of the I585I/V genotype and TRPA1 expression on asthma symptom control as a function of tobacco smoke exposure among children with asthma.

Materials and Methods

Chemicals and Other Materials

N-(4-*tert*-butylbenzyl)-*N*-(1-[3-fluoro-4-(methylsulfonylamino)-phenyl]ethyl)thiourea (LJO-328) was provided by J. Lee of Seoul National University. The structure has been published.[29] 2-Mercaptoethanol, *n*-vanillylnonanamide (nonivamide; a capsaicin analog), allyl isothiocyanate (AITC), ionomycin calcium salt, and phorbol 12-myristate 13-acetate (PMA) were from Sigma-Aldrich. Dimethyl sulfoxide (DMSO) was from Fisher Scientific. BMS-345541 and Go6983 were from Tocris, and recombinant human tumor necrosis factor-alpha (TNFα), interleukin-1 alpha (IL1α), IL1β, IL6, and IL13 were from Peprotech. 4-(4-Fluorophenyl)-2-(4-nitrophenyl)-5-(4-pyridyl)-1H-imidazole (PD169316) was from Cayman Chemical.

WSPM, DEP, and CFA

Preparation of pine WSPM,[6] and the sources and properties of the DEP[4,5] and CFA[3] have been described. Briefly, WSPM was prepared by burning ∼10 g of Austrian pine (from a tree growing in the Salt Lake Valley; 1.5 cm long × 0.2–0.5 cm wide) using a pipe furnace at 750°C with constant air flow. WSPM was collected using an Anderson cascade impactor operated at 1 L/min, and fractions 6 and 7 (0.65–1.1 μm and 0.43–0.65 μm) were used. For experiments, WSPM concentrate was suspended in DMSO at 115 mg/mL and diluted to 0.076 mg/mL in media containing ≤0.2% DMSO to achieve a 20-μg/cm^2 area dose in a single well of a 6-well plate. Features of pine WSPM, and the effects that it has on AECs (i.e., calcium flux, pro-inflammatory, cytostatic, and cytotoxic) have been described.[24,25,30,31] Specifically, the material was shown to contain TRPA1 agonists, including resin acids, perinaphthenone, coniferaldehyde, ethyl phenols, and substituted xylenols; ethyl phenols and xylenols also activate TRPV3.[6,30] The DEP was collected from idling diesel-powered vehicles during emissions testing in the Salt Lake City area.[4] The PM was suspended in media containing ≤0.2% DMSO and applied to cells at a final area dose of 10 μg/cm^2. The DEP used in this study was shown to contain the TRPA1 agonists 2,4-di-*tert*-butylphenol (also a TRPV3 agonist) and several quinones (benzo and naptho), as well as perinanpthenone.[4] Finally, CFA was collected from the Hunter power plant in Castle Dale, Utah, and fractionated to <10 μm. The ash was from low-sulfur bituminous coal, which was previously reported to consist of primarily insoluble oxides and salts of silicon, calcium, aluminum, and iron, with ∼3% elemental carbon and ∼1% unspecified organic carbon[32] (presumably polycyclic aromatic hydrocarbons as described for other CFA samples[33]). Effects of CFA on AECs and TRP channels have also been described.[3,26,34]

Cell Culture

BEAS-2B and HEK-293 cells were from ATCC. These and other cells were maintained in a humidified cell culture incubator at 37°C with a 95% air:5% carbon dioxide (CO_2) atmosphere. Human TRPV1-overexpressing HEK-293 and BEAS-2B cells were generated as previously described.[15,35] Briefly, cells were transfected with a pcDNA3.1 plasmid (ThermoFisher) harboring human TRPV1, selected using Geneticin (300 μg/mL), and expanded from a single colony. Overexpression was verified using calcium flux assays and western blots. TRPV1-overexpressing HEK-293 cells were cultured in Dulbecco's Modified Eagle Medium/Ham's F12 (DMEM:F12) media containing 5% fetal bovine serum, 1× penicillin/streptomycin, and 300 μg/mL Geneticin (ThermoFisher), and BEAS-2B cells were cultured in LHC-9 medium fortified with 300 μg/mL Geneticin. Normal (NHBE; CC-2540 and CC-2541) and diseased (DHBE; CC-2540 and 00194911) human bronchial epithelial cells (HBEs) were from Lonza and were cultured in bronchial epithelial cell growth medium (Lonza). NHBEs immortalized with cyclin-dependent kinase 4 (CDK4) and telomerase reverse transcriptase (hTERT), or HBEC3-KT cells, were from ATCC (CRL-4051) and were grown in airway epithelial cell basal medium supplemented with bronchial epithelial cell growth kit, 30 μg/mL Geneticin, and 250 ng/mL puromycin (ATCC). Human small airway epithelial cells (SAECs; CC-2547) were from Lonza and were grown in BronchiaLife epithelial airway medium complete kit.

Cell Genotyping

NHBE and DHBE cells were genotyped using TaqMan Genotyping Master Mix and assays for *TRPV1* I585V (ThermoFisher #C_11679656_10) I315M (ThermoFisher #C_1093688_10), T469I (ThermoFisher #C_1093674), *TRPA1* R3C (ThermoFisher #C_2175739_10), and R58T (ThermoFisher #C_25646603_10). Genomic DNA was isolated from cells using the GeneElute Mammalian Genomic DNA Miniprep Kit (Sigma-Aldrich). DNA was then quantified by ultraviolet (UV) absorbance on a Nanodrop One^c (ThermoFisher) and assayed using a Life Technologies QuantStudio 6 Flex instrument (ThermoFisher) and the polymerase chain reaction (PCR) program specified by the supplier for the TaqMan Genotyping Master Mix. Genotypes were differentiated by relative probe fluorophore intensity using pcDNA3.1 plasmids harboring human *TRPV1*, human *TRPA1*, and the target single nucleotide polymorphism (SNP) variant mutations.[15,26] Genotyping results and donor lot identifications for the cells used in this work are provided in Table S1. HBEC3-KT cells have the *TRPV1* I585I/V genotype, BEAS-2B cells the I585I/I genotype, SAECs the I585I/V genotype, and NHBEs have variable genotypes.

Quantitative Real-Time PCR

Cells were plated at 10,000 cells/cm^2 in 6-well plates and treated at ∼90% confluence (3 d post plating with feeding on day 2). After treatment, total RNA was isolated using the PureLink RNA Mini Kit (Invitrogen). Total RNA (2 μg) was quantified by UV absorbance on a Nanodrop One^c (ThermoFisher) and complementary DNA (cDNA) was synthesized using the ABI High-Capacity cDNA Synthesis Kit with RNase inhibitor (Applied Biosystems). The cDNA was then subjected to analysis by quantitative real-time PCR (q-PCR) using TaqMan Gene Expression Master Mix (ThermoFisher) and a Life Technologies QuantStudio 6 Flex instrument. The following TaqMan probe-based assays were used: human glyceraldehyde 3-phosphate dehydrogenase (*GAPDH*; Hs99999905_m1), human *TRPA1* (Hs00175798_m1), human *TRPV1* (Hs00218912_m1), human *TRPV3* (Hs00376854_m1), human *NLRP2* (Hs01546932_m1), human *IGFBP2* (Hs01040719_m1), human DNA damage-inducible transcript-3 (*DDIT3*; Hs_00358796_g1), and human interleukin-8 (*IL8*; Hs00174103_m1). The PCR programs used were according to the supplier for the TaqMan Gene Expression Master Mix and probe assays. mRNA expression was normalized to the housekeeping gene, human β2-microglobulin (*β2M*; Hs00984230_m1), and the average value of control samples (i.e., the comparative ΔΔCt method)[36] with relative quantification (Rq) reported.

Small Interfering RNA Studies

Small interfering RNA (siRNA) transfections were performed according to the ThermoFisher Stealth/siRNA Transfection Lipofectamine 2000 Protocol. HBEC3-KT cells were plated in 6-well plates at $\sim 5{,}000\,\text{cells}/\text{cm}^2$ and transfected with siRNA at 30%–50% confluence (2 d post plating), as per the manufacturer protocol. Briefly, siRNAs were reconstituted to a concentration of $50\,\text{pmol}/\mu\text{L}$ in nuclease-free water. An aliquot containing 100 or $500\,\text{pmol}/\text{mL}$ negative control (Silencer Negative Control siRNA No.1; ThermoFisher #AM4611), positive control *GAPDH* (ThermoFisher #4404024), *NLRP2* siRNA-1 or -2 (ThermoFisher siRNA ID 25505; AM16708), or *TRPV1* siRNA (ThermoFisher siRNA ID 105495; AM16708) was diluted in antibiotic and serum-free HBEC3-KT media and incubated in the dark at room temperature. After 5 min, the siRNA was mixed 1:1 with the diluted Lipofectamine 2000 and incubated for 25 min in the dark at room temperature. After incubation, the siRNA:Lipofectamine complex was diluted with 700 μL of antibiotic-free and serum-free HBEC3-KT media to a final volume of 1 mL. This solution was then added to an individual well in a 6-well plate and incubated for 6 h, upon which the transfection solution was replaced with fresh HBEC3-KT media. Isolation and quantification of mRNA after siRNA transfection was performed as described above, 24 h posttransfection. For western blotting, cells were plated at $\sim 5{,}000\,\text{cells}/\text{cm}^2$ in 75-cm^2 flasks and the siRNA volumes and concentrations were adjusted according to the supplier protocol.

Western Blotting

Western blots were performed as previously described by Nguyen et al.[25] For isolating nuclear protein, the NE-PER Nuclear and Cytoplasmic Extraction Reagents kit and protocol (ThermoFisher) was used. Cells were grown to confluence in 75-cm^2 flasks. Total protein was harvested on ice using radioimmunoprecipitation buffer, supplemented with 6 M urea, 1% sodium dodecyl sulfate, and Halt protease inhibitor. Lysates were sonicated on ice using $10\times$ 1-s pulses at 100 W, repeated 10 times and clarified by centrifugation at $13{,}000\times g$ for 15 min at 4°C. Protein concentrations were determined using the bicinchoninic acid protein assay kit (ThermoFisher), and 30 μg was loaded into each well of a 4%–12% Bolt Bis-Tris 12-well gel and resolved by electrophoresis for 1.5 h at 120 V. The Precision Plus Protein Dual Color Standards (5 μL) ladder was also used (BioRad). Following electrophoresis, the proteins were transferred to a polyvinylidene fluoride membrane using the iBlot 2 gel transfer device. After transfer, the membrane was incubated in SuperBlock (ThermoFisher) for 1 h at room temperature. Primary rabbit monoclonal antibodies against nuclear factor kappa light chain enhancer of activated B cells (NF-κB)/p65 (#3034; Cell Signaling Technology) and NF-κB-phospho-S536 (#3033; Cell Signaling Technology) were used at 1:5,000 dilution. Polyclonal antibodies against NLRP2 (ThermoFisher #15182-1-AP) and rabbit nuclear matrix protein (p84; ThermoFisher, PA5-69083) were used at 1:1,000 dilution. A mouse monoclonal antibody against β-actin (8H10D10; Cell Signaling Technology #3700) was used at 1:10,000 dilution. Rabbit GAPDH (D16H11) monoclonal antibody (Cell Signaling Technology #5174) was used at 1:1000 dilution. All primary antibodies were prepared in 5% bovine serum albumin with 0.1% sodium azide and incubated with the membranes at 4°C for 16 h. Horseradish peroxidase-conjugated sheep-antimouse (NA931) and anti-rabbit (NA934) secondary antibodies (GE Health Sciences) were used at 1:10,000 in SuperBlock and were also applied for 16 h at 4°C. SuperSignal West Dura Extended Duration Substrate (ThermoFisher) was added to the membrane and visualized using a FluorChem M imager with the chemiluminescence plus markers setting. Bands were quantified using densitometry analysis of 8-bit images in ImageJ[37] and normalized to the respective gene, as outlined in the figure legends.

RNA Sequencing

RNA sequencing was performed as previously described[15] at the High Throughput Genomics Core Facility at the Huntsman Cancer Institute, University of Utah. NHBE cells from the four donors (14359 and 14664 for *TRPV1* I585I/I, and 9853 and unknown for *TRPV1* I585I/V) were used. Total RNA was extracted using the RNeasy Mini kit (Qiagen) with on-column DNase digestion. RNA quality was assessed by RNA nanochip technology, and library construction was performed using the Illumina TruSeq Stranded mRNA Sample Preparation kit using established protocols. The sequencing libraries (18 pM) were then chemically denatured and applied to an Illumina TruSeq version 3 single-read flow cell using an Illumina cBot. Hybridized molecules were clonally amplified and annealed to sequencing primers with reagents from an Illumina TruSeq SR Cluster kit, version 3-cBot-HS. Following transfer of the flow cell to an Illumina HiSeq instrument, a 50-cycle single-read sequence run was performed using TruSeq SBS version 3 sequencing reagents. Data were processed at the University of Utah Bioinformatics core. The data presented in this publication have been deposited in the National Center for Biotechnology Information's (NCBI's) Gene Expression Omnibus (GEO) and are accessible through GEO Series accession no. GSE85447 (https://www.ncbi.nlm.nih.gov/geo/query/acc.cgi?acc=GSE85447).

Calcium Flux/TRP Activity Assays

Calcium flux in HBEC3-KT cells was measured using the Fluo-4 Direct assay kit and imaging on an EVOS FL Auto microscope at $10\times$ magnification using a green fluorescent protein (GFP) filter.[3–5,25,26,30] Briefly, cells were plated in a flat-bottom 96-well plate at $\sim 10{,}000\,\text{cells}/\text{cm}^2$, fed on day 2 post plating, and assayed at 80%–90% confluence 3 d post plating. Pretreatment of cells with nonivamide (10 μM), LJO-328 (25 μM), pine WSPM ($20\,\mu\text{g}/\text{cm}^2$), TNFα (50 ng/mL), and BMS-345541 (10 μM) occurred 12 or 24 h before the assay. Prior to the assay, the cells were loaded with $1\times$ Fluo-4 diluted 1:1 in LHC-9 at 37°C for 1 h. After 1 h, the Fluo-4 was removed and the cells were washed with LHC-9 containing 1 mM probenecid and 0.75 mM trypan red (ATT Bioquest). The assays were performed in an on-stage environmental chamber maintained at 37°C in a 95% air:5% CO_2 atmosphere. Agonist treatments (AITC 25 or 150 μM) were added to cells at $3\times$ the desired final concentration in LHC-9, which contained 111.1 μM calcium. Images were captured every 6 s for 72 s. Changes in fluorescence were quantified using a custom MATLAB program, as previously described.[3,5] Reported values are from the 60-s time point and were corrected by subtracting the fluorescence response to a blank media control (i.e., no agonist) and then normalized to the response value at 72 s following ionomycin (10 μM) treatment applied after the 60-s image was taken.

Calcium flux in HEK-293 cells stably overexpressing TRPV1 (HEKV1OE cells) was measured essentially as above using a BMG Labtech NOVOStar fluorescence plate reader. The following differences applied: HEKV1OE cells were plated in flat-bottom 96-well plates coated with 1% gelatin at $\sim 30{,}000$ cells/well and assayed at 100% confluence 1–2 d post plating. Pretreatments (12 h) included Go6983 (10 μM) or media containing $\leq 0.2\%$ DMSO (control). Changes in fluorescence were determined using the NOVOStar analysis software (MARS version 2.41). The values were normalized to the response elicited by LHC-9 media and are reported as the maximum change in fluorescence intensity from plots of change in fluorescence vs. time (60 s total assay time).

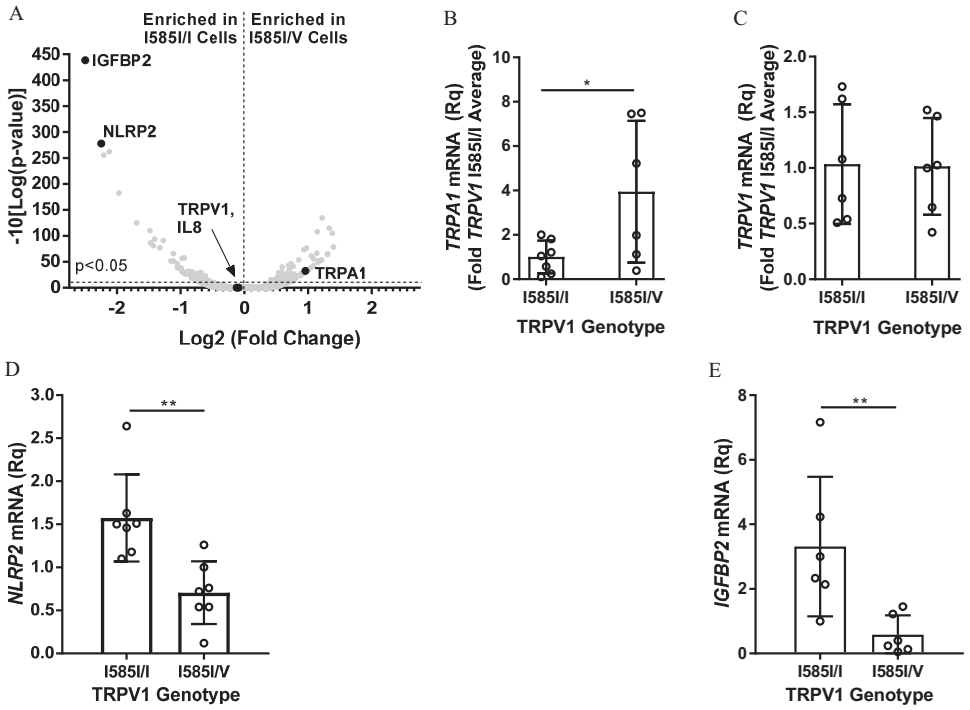

Figure 1. (A) Volcano plot of RNA sequencing data from NHBE cells with either the *TRPV1* I585I/I or I585I/V genotypes. Summary data can be found in Excel Table S1. (B) *TRPA1*, (C) *TRPV1*, (D) *NLRP2*, and (E) *IGFBP2* mRNA expression in NHBE cells having either the *TRPV1* I585I/I or I585I/V genotype ($n=6$ or 7 donors/genotype). Data (Rq) are the mean ± SD, relative to $\beta 2M$ mRNA and the average for target gene expression in NHBEs with the I585I/I genotype. $^{*}p \leq 0.05$ and $^{**}p < 0.01$ using a one-tailed unpaired Student's *t*-test. Summary data can be found in Excel Table S2 (B,C) Excel Table S3 (D,E). Note: IGFBP2, insulin like growth factor binding protein 2; NHBE, normal human bronchial epithelial (cells); NLRP2, nucleotide-binding oligomerization domain, leucine rich repeat and pyrin domain containing 2; Rq, relative quantification; SD, standard deviation; TRPA1, transient receptor potential cation channel subfamily A member 1; TRPV1, transient receptor potential cation channel subfamily V member 1; $\beta 2M$, β2-microglobulin.

Asthma Cohort Studies

Details on the cohort used in this study have been published,[15,26,38] and updated demographic and other information relevant to asthma are summarized in Table S2. Briefly, participants were recruited from the emergency department and inpatient wards at Primary Children's Hospital, University of Utah, Salt Lake City, Utah, as part of an institutional review board–approved study of factors influencing asthma symptom control. All patients/parents/guardians provided informed consent prior to enrollment, DNA sampling, and data collection and analysis. Saliva samples were obtained prospectively from children 2–17 years of age with a

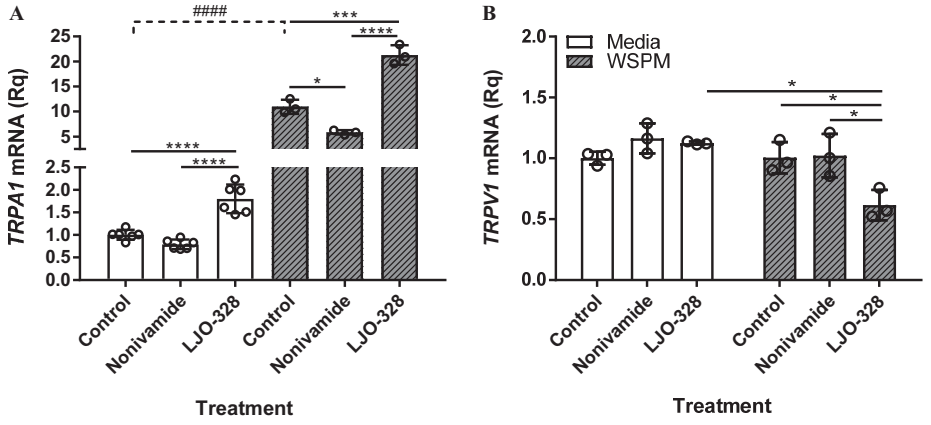

Figure 2. (A) *TRPA1* and (B) *TRPV1* mRNA expression in HBEC3-KT cells following 24-h treatment with nonivamide (10 μM) or LJO-328 (25 μM; white bars), and co-treatment with pine WSPM in media (20 μg/cm^2; gray hashed bars). Data (Rq) are the mean ± SD for target gene mRNA expression relative to $\beta 2M$ mRNA and cells treated with media containing 0.2% DMSO only ($n=3$–6). Control and WSPM co-treated groups were analyzed independently comparing all treatment groups using one-way ANOVA and Tukey's multiple comparisons test. $^{*}p \leq 0.05$, $^{***}p < 0.001$, and $^{****}p < 0.0001$. $^{\#\#\#\#}$Indicates significant difference ($p < 0.0001$) from all WSPM co-treated groups using two-way ANOVA and a Bonferroni multiple comparisons test comparing the corresponding ± WSPM groups. Summary data can be found in Excel Table S4. Note: ANOVA, analysis of variance; DMSO, dimethyl sulfoxide; HBEC3-KT, telomerase reverse transcriptase and CDK4–immortalized normal human bronchial epithelial (cells); LJO-328, *N*-(4-*tert*-butylbenzyl)-*N*-(1-[3-fluoro-4-(methylsulfonylamino) phenyl]ethyl)thiourea; nonivamide, 2-mercaptoethanol, *n*-vanillylnonanamide; Rq, relative quantity; SD, standard deviation; TRPA1, transient receptor potential cation channel subfamily A member 1; TRPV1, transient receptor potential cation channel subfamily V member 1; WSPM, wood smoke particulate matter; $\beta 2M$, β2-microglobulin.

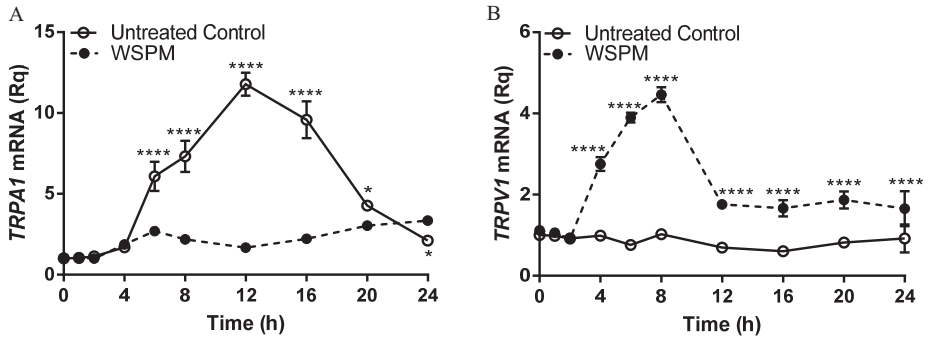

Figure 3. Temporal changes in (A) *TRPA1* and (B) *TRPV1* mRNA expression in HBEC3-KT cells following treatment with media containing 0.2% DMSO (open circles, solid lines) or pine WSPM in media (20 μg/cm^2; closed circles, dashed lines). Data (Rq) are the mean ± SD for target gene mRNA expression relative to *β2M* mRNA and the control ($n = 3$). $^{*}p \leq 0.05$ and $^{****}p < 0.0001$ using repeated measures two-way ANOVA comparing the control and WSPM-treated groups at each time and correction using Bonferroni's multiple comparisons test. Summary data can be found in Excel Table S6. Note: ANOVA, analysis of variance; DMSO, dimethyl sulfoxide; HBEC3-KT, telomerase reverse transcriptase and CDK4–immortalized normal human bronchial epithelial (cells); Rq, relative quantification; SD, standard deviation; TRPA1, transient receptor potential cation channel subfamily A member 1; TRPV1, transient receptor potential cation channel subfamily V member 1; WSPM, wood smoke particulate matter; *β2M*, β2-microglobulin.

physician-confirmed diagnosis of asthma. Information on chronic medical conditions, concomitant medication use, and the chief complaint at the time of enrollment was collected during enrollment and subsequent medical chart abstraction. The level of asthma control in each subject was assessed using a questionnaire based on guidelines modified from the National Heart, Lung, and Blood Institute's Expert Panel Report 3[39] (Table S3), as described by Stockman et al.[38] The questionnaire consisted of five questions scored on a four-point scale (i.e., 0, 1, 2 or 3). The asthma control score equals the sum of the five item scores, where 0 represents well controlled and 15 represents poorly/not controlled.

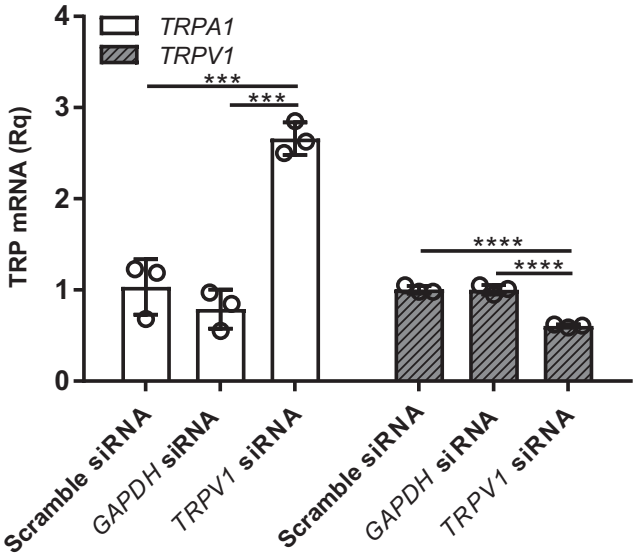

Figure 4. *TRPA1* (white bars) and *TRPV1* (gray hashed bars) mRNA expression in HBEC3-KTs transfected with scramble, *GAPDH*, and *TRPV1* siRNA (500 pmol/mL) 24 h posttransfection. Data (Rq) are the mean ± SD for target gene mRNA expression relative to *β2M* mRNA and the average for cells transfected with scramble siRNA ($n = 3$). Data for TRPA1 and TRPV1 were analyzed independently comparing all three siRNAs using one-way ANOVA and Tukey's multiple comparisons test. $^{***}p < 0.001$ and $^{****}p < 0.0001$. Summary data can be found in Excel Table S7. Note: ANOVA, analysis of variance; GAPDH, glyceraldehyde 3-phosphate dehydrogenase; HBEC3-KT, telomerase reverse transcriptase and CDK4–immortalized normal human bronchial epithelial (cells); Rq, relative quantification; SD, standard deviation; siRNA, small interfering RNA; TRP, transient receptor potential; TRPA1, transient receptor potential cation channel subfamily A member 1; TRPV1, transient receptor potential cation channel subfamily V member 1; *β2M*, β2-microglobulin.

Saliva Collection, Genomic DNA Extraction, and SNP Genotyping

DNA was collected using either an Oragene DNA Kit (DNA Genotek) or Zymo DNA/RNA shield collection tube with swab (Zymo Research) and extracted using the GeneElute Mammalian Genomic DNA Miniprep Kit (Sigma-Aldrich). DNA was then quantified by Nanodrop and assayed for TRP SNPs using custom 64- or 128-feature TaqMan Open Array cards (ThermoFisher) containing assays for the *TRPV1* I315M, T469I, I585V, and *TRPA1* R3C and R58T SNPs, among others, at the University of Utah Genomics core facility. Prior to genotyping, 4 ng of genomic DNA was amplified using a custom TaqMan PreAmp Mastermix specific to the array card features. The TaqMan reactions were cycled as recommended by the manufacturer on a Life Technologies QuantStudio 12K instrument. Data clustering and SNP identification analysis were performed using TaqMan Genotyper software (v1.3.1; Life Technologies).

Statistical Analysis and Graphics

Graphing and statistical analyses were performed using GraphPad Prism (version 7.03). Values are represented as the mean ± standard deviation (SD). One-tailed unpaired Student's *t*-tests; one-way analysis of variance (ANOVA) and Tukey's multiple comparisons test; two-way ANOVA and either a Bonferroni, Tukey's, or Dunnett's multiple comparisons test; and repeated measures two-way ANOVA and Bonferroni's multiple comparisons test were used as specified in the figure legends. A *p*-value of ≤0.05 was considered significant for all experiments. Schematics were prepared using Adobe Illustrator (v24.4.8).

Results

TRPA1 *mRNA Expression in AECs with the* TRPV1 *I585I/V Genotype*

Transcriptome analysis comparing NHBEs with either the *TRPV1* I585I/I or I585I/V genotype revealed an enrichment of *TRPA1* mRNA in cells with the I585I/V genotype (Figure 1A), as previously reported.[15] Using 13 unique donor lots of NHBEs and qPCR, cells with the *TRPV1* I585I/I genotype expressed on average 3.9-

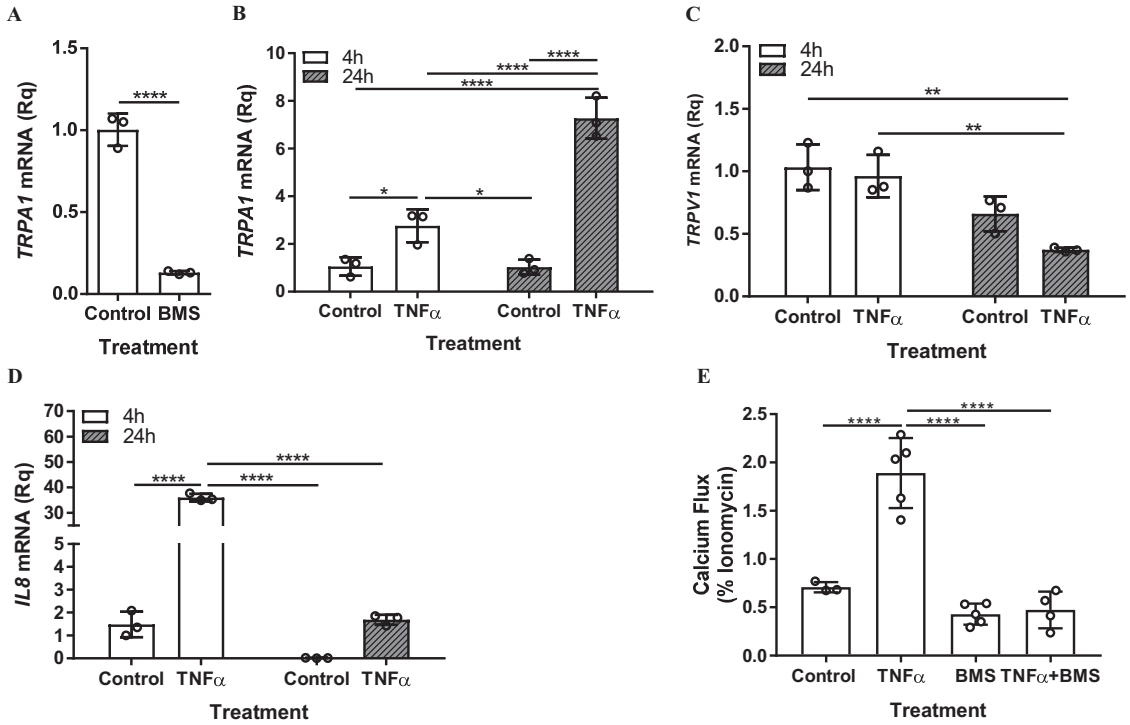

Figure 5. (A) *TRPA1* mRNA expression in HBEC3-KT cells following 24-h treatment with media containing 0.2% DMSO or the NF-κB inhibitor BMS-345541 (BMS; 10 μM). $^{****}p < 0.0001$ using a one-tailed unpaired Student's *t*-test. (B) *TRPA1*, (C) *TRPV1*, and (D) *IL8* mRNA expression in HBEC3-KT cells following 4- and 24-h treatment with TNFα (50 ng/mL) or 0.01% BSA in media ($n = 3$). Data (Rq) are the mean ± SD for target gene mRNA expression relative to *β2M* mRNA and the control. $^{*}p \leq 0.05$, $^{**}p < 0.01$, and $^{****}p < 0.0001$ using two-way ANOVA and Tukey's multiple comparisons test comparing all treatments groups. (E) Calcium flux in HBEC3-KT cells treated for 24 h with either media containing 0.01% BSA and 0.2% DMSO, TNFα (50 ng/mL), BMS-345541 (10 μM), or TNFα and BMS subsequently stimulated by the addition of AITC (150 μM). Data were normalized to ionomycin ($n = 5$). Raw images are shown in Figure S6. $^{****}p < 0.0001$ using one-way ANOVA and Tukey's multiple comparison test comparing all groups. Summary data can be found in Excel Table S8. Note: AITC, allyl isothiocyanate; ANOVA, analysis of variance; BSA, bovine serum albumin; DMSO, dimethyl sulfoxide; HBEC3-KT, telomerase reverse transcriptase and CDK4–immortalized normal human bronchial epithelial (cells); IL8, interleukin-8; NF-κB, nuclear factor kappa light chain enhancer of activated B cells; Rq, relative quantification; SD, standard deviation; TNFα, tumor necrosis factor-alpha; TRPA1, transient receptor potential cation channel subfamily A member 1; TRPV1, transient receptor potential cation channel subfamily V member 1; *β2M*, β2-microglobulin.

fold ($p = 0.0183$) lower *TRPA1* mRNA than cells with the I585I/V genotype, whereas *TRPV1* was equivalent (Figure 1B,C). Stratification of these data based on the *TRPV1* I315M and T469I SNPs demonstrated essentially no difference in *TRPA1* mRNA expression, but *TRPV1* mRNA was on average 1.8-fold ($p = 0.0083$) more abundant in cells with the *TRPV1* T469I/T genotype (Figure S1). Agreement between changes in *TRPA1* and *TRPV1* mRNA and activity/protein in lung epithelial cells has previously been shown.[15,25,29,40] In cells with the *TRPV1* I585I/I genotype, mRNA for the NF-κB-induced and NF-κB regulatory genes *NLRP2*[41,42] and *IGFBP2*[43–45] were enriched; *NLRP2* and *IGFBP2* mRNA expression was 2.2- ($p = 0.0016$) and 5.7-fold ($p = 0.0070$) lower in cells with the *TRPV1* I585I/V genotype compared with cells with the I585 I/I genotype (Figure 1D,E).

Effect of TRPV1 Activity on TRPA1 *mRNA Expression*

The role of variable TRPV1 activity as a basis for differences in *TRPA1* mRNA expression was tested by treating HBEC3-KT cells for 24 h with the TRPV1 agonist nonivamide (more active TRPV1, akin to TRPV1 I585I/I) or the antagonist LJO-328 (less active TRPV1, akin to TRPV1 I585I/V). Protracted stimulation of TRPV1 with nonivamide lowered *TRPA1* mRNA expression 1.3-fold ($p = 0.1997$) compared with media + DMSO-treated control cells, whereas 1.8-fold higher *TRPA1* mRNA expression ($p < 0.0001$) was observed when TRPV1 was inhibited by LJO-328 (Figure 2A, white bars). The difference between nonivamide and LJO-328 treatment was 2.3-fold ($p < 0.0001$) and *TRPV1* mRNA expression was not different between cells treated with nonivamide and those treated with LJO-328 (Figure 2B, white bars). Similar differences in *TRPA1* mRNA expression were observed using TRPV1-overexpressing BEAS-2B cells (Figure S2); cells treated with nonivamide had 5.1-fold lower *TRPA1* mRNA expression ($p = 0.6425$) and cells treated with LJO-328 had 12.5-fold higher expression ($p < 0.0001$).

TRPA1 *mRNA Expression and Effects of TRPV1 Agonists and Antagonists on AECs Treated with Pro-Inflammatory and Cytotoxic Agents*

The effects of concurrent treatment of cells with pine WSPM, a pro-inflammatory and pneumotoxic environmental pollutant that activates TRPA1,[6,24,25] on the ability of TRPV1 agonists and antagonists to alter *TRPA1* mRNA expression was also evaluated. HBEC3-KT cells exposed to WSPM (24 h) alone had 10.9-fold higher *TRPA1* mRNA expression ($p < 0.0001$; Figure 2A, gray hashed bars). As above, cells co-treated with nonivamide and WSPM had ∼1.9-fold lower *TRPA1* mRNA expression ($p < 0.0102$), whereas cells co-treated with LJO-328 and WSPM had 1.9-fold higher expression ($p < 0.0003$; Figure 2A, gray hashed bars). Also as above, *TRPV1* mRNA expression was similar to control cells for cells co-treated with nonivamide and WSPM, but it was 1.6-fold lower ($p = 0.0396$) in cells co-treated with LJO-328 and WSPM (Figure 2B, gray hashed bars). Cells were also treated with alternative inflammatory stimuli, including TNFα, IL1α, IL1β, IL6, and IL13. Cells treated with all but IL13 had

~1.5- to 2-fold higher *TRPA1* mRNA expression 4 h posttreatment (Figure S3).

TRP mRNA Expression with WSPM/TRPA1 Agonist Challenge

The temporal profiles of *TRPA1* and *TRPV1* mRNA expression following WSPM treatment were distinct and opposite (Figure 3A, B), revealing an inverse relationship. As previously observed,[25] *TRPA1* mRNA increased in control cells provided fresh media at time = 0, between 6 and 20 h. This did not occur with WSPM treatment. Accordingly, *TRPA1* mRNA was markedly lower relative to the media-treated control cells when normalized at each time point. However, after ~24 h, as the WSPM-treated cells visibly recovered from stress/damage and restored a monolayer, *TRPA1* mRNA was higher (1.6-fold; $p = 0.0131$) compared with control cells, as in Figure 2A. The suppression of *TRPA1* mRNA expression was also observed in cells treated with the TRPA1 agonists AITC, coniferaldehyde, and 2,4-di-*tert*-butylphenol (Figure S4), albeit the magnitude and duration of the effect varied by treatment, with WSPM producing the most robust effect and monolayer damage. Concurrently, *TRPV1* mRNA was higher in cells treated with WSPM between 0 and 24 h (Figures 3B and S4), and similar time-dependent perturbations to mRNA expression for *TRPV3* (higher expression across at all time points where *TRPA1* was lower, similar to *TRPV1*), *TRPV4* (higher expression at 0 to 8 h and lower at other times), and *TRPM8* (lower at all time points up to 24 h, paralleling *TRPA1*) following WSPM treatment and treatment with other TRPA1 agonists. Like *TRPA1* and *TRPV1*, variations in *TRPV3* mRNA also manifest as changes in protein expression and activity.[25,31]

TRPA1 *mRNA Expression in Cells with Suppression of TRPV1 Expression/Function Using siRNA*

To further link TRPV1 expression/function with *TRPA1* mRNA expression, *TRPV1* siRNA was used. Cells treated with *TRPV1* siRNA had 2.7- ($p < 0.004$) and 3.4-fold ($p = 0.002$) higher *TRPA1* mRNA compared with the scramble and *GAPDH* siRNA controls, respectively (Figure 4, white bars). In this experiment, *TRPV1* mRNA was ~1.6-fold ($p = 0.0151$) lower relative to both controls ($p < 0.0001$ for both, gray hashed bars). For comparison, cells treated with *GAPDH* siRNA had 6.3-fold ($p < 0.0001$) and ~1.5-fold ($p = 0.0023$) lower *GAPDH* mRNA and protein expression (Figure S5).

NF-κB and TRPA1, TRPV1, *and IL8 mRNA Expression*

A role for NF-κB in regulating *TRPA1* mRNA expression was tested by treating HBEC3-KT cells (24 h) with the Inhibitor of Nuclear Factor Kappa-B Kinase Subunits Alpha and Beta (IKKα/IKKβ; NF-κB pathway) inhibitor BMS-345541. Treated cells had 7.7-fold ($p < 0.0001$) lower *TRPA1* mRNA expression compared with control cells (Figure 5A). Alternatively, cells treated with TNFα, an NF-κB pathway activator, had 2.6- ($p = 0.0353$) and ~6.9-fold ($p = 0.0001$) higher *TRPA1* mRNA expression at 4 and 24 h, respectively (Figure 5B). Consistent with the inverse relationship between *TRPA1* and *TRPV1* mRNA expression, cells treated with TNFα expressed lower *TRPV1* mRNA with time (1.8-fold lower with 24-h treatment; $p = 0.1425$; Figure 5C), consistent with reports that NF-κB inhibits TRPV1 expression.[46] Simultaneously mRNA for another NF-κB target gene, *IL8*,[47,48] was 24.3-fold ($p < 0.0001$) and 140.4-fold ($p = 0.1241$) higher at 4 and 24 h, respectively (Figure 5D). TRPA1 activity was also higher in HBEC3-KT cells treated for 24 h with TNFα, as indicated by 2.7-fold higher AITC-induced changes in intracellular calcium ($p = 0.0001$; Figure 5E). In addition, pretreatment with BMS-345541 alone and in combination with TNFα, resulted in ~1.6-fold ($p = 0.3787$) and ~1.4-fold ($p = 0.5550$) lower AITC-induced calcium flux relative to the control, as well as 4.4- ($p < 0.0001$) and 4-fold ($p = 0.0001$) lower response compared with TNFα-treated cells. Figure S6 shows raw images and antagonist inhibition data confirming that the AITC-induced calcium flux was due to TRPA1.

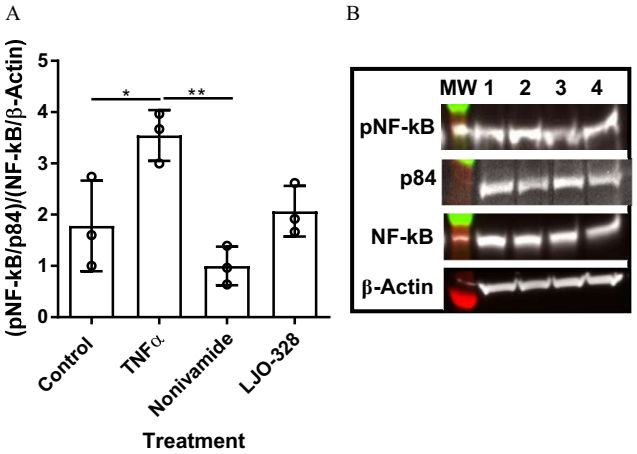

Figure 6. (A) Quantification of nuclear pNF-κB/p65 in HBEC3-KTs treated for 24 h with media, TNFα (50 ng/mL), nonivamide (10 μM), or LJO-328 (25 μM). pNF-κB/p65 intensity was normalized to p84, and NF-κB (total) was normalized to β-actin prior to calculating the pNF-κB/NF-κB ratio. Data represents the mean ± SD ($n = 3$). $^{**}p < 0.01$ using one-way ANOVA and Tukey's multiple comparisons test comparing all groups. (B) Representative western blot image where, from left to right, are the molecular weight standard (MW), control (1), TNFα (2), nonivamide (3), and LJO-328 treatments (4). Raw western blot data are shown in Figure S7. Summary data can be found in Excel Table S9. Note: ANOVA, analysis of variance; HBEC3-KT, telomerase reverse transcriptase and CDK4–immortalized normal human bronchial epithelial (cells); LJO-328, *N*-(4-*tert*-butylbenzyl)-*N*-(1-[3-fluoro-4-(methylsulfonylamino)phenyl]ethyl)thiourea; nonivamide, 2-mercaptoethanol, *n*-vanillylnonanamide; NF-κB, nuclear factor kappa light chain enhancer of activated B cells; p84, rabbit nuclear matrix protein; pNF-κB, phospho-nuclear factor kappa light chain enhancer of activated B cells; SD, standard deviation; TNFα, tumor necrosis factor-alpha.

Nuclear Localization of NF-κB/p65 and TRPA1 *mRNA Expression*

Nuclear localization of NF-κB is central to transcriptional regulation by NF-κB.[49] Western blot analysis of NF-κB proteins from HBEC3-KTs treated with TNFα, nonivamide, and LJO-328 showed 2-fold ($p = 0.0275$) higher nuclear phospho-NF-κB (pNF-κB) with TNFα treatment and 1.8 ($p = 0.4248$) lower and essentially equivalent (i.e., 1.2-fold; $p = 0.9333$) nuclear pNF-κB with nonivamide and LJO-328 treatment, respectively (Figure 6A,B), consistent TRPV1-dependent modulation of NF-κB to alter TRPA1 expression. Unprocessed western blot images are shown in Figure S7.

Relationship between Protein Kinase C, p38 Mitogen-Activated Protein Kinase, and TRPA1 *mRNA Expression*

Protein kinase C (PKC)[50] and p38 mitogen-activated protein kinase (MAPK)[51,52] promote NF-κB pathway activity and enhance target gene (e.g., IL8) expression.[47,48] PKC also acutely sensitizes TRPV1.[53,54] HBEC3-KTs cells treated with the PKC activator and TRPV1 sensitizer PMA exhibited dose- and time-dependent lower *TRPA1* mRNA expression at 4 and 12 h (Figure 7A) while simultaneously exhibiting higher *TRPV1* and *IL8* mRNA expression at 4 h, but less so at 12 h (Figure 7B,C).

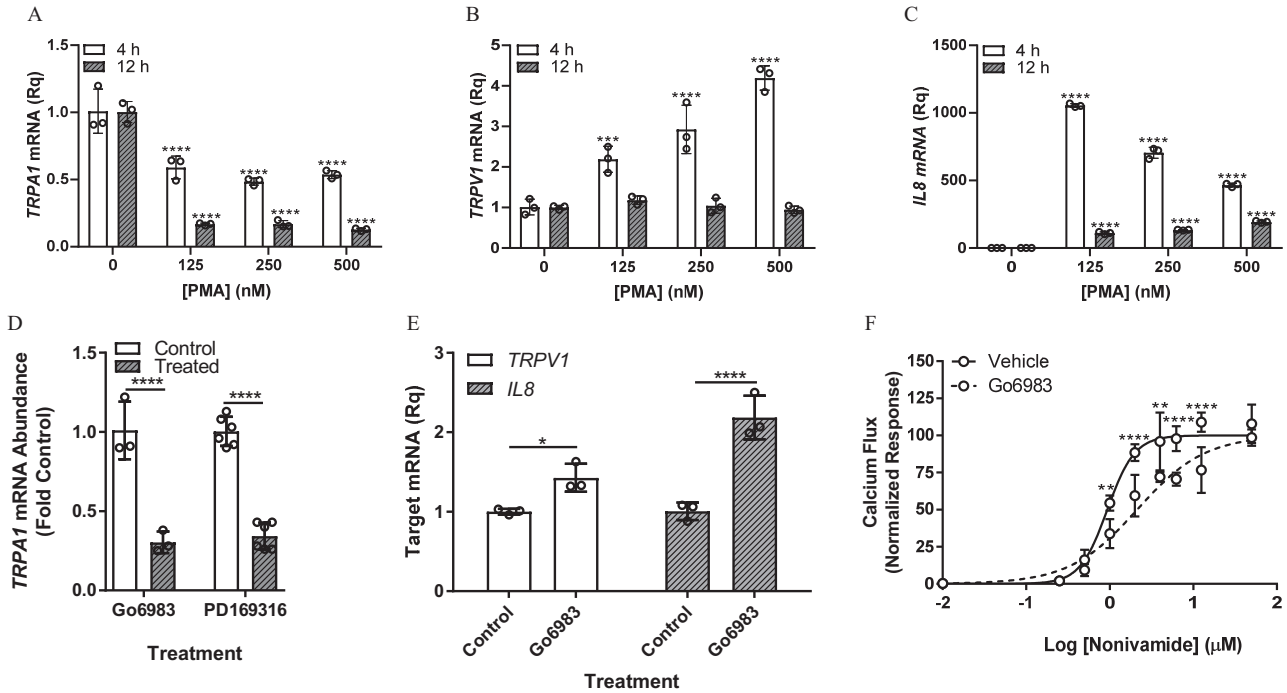

Figure 7. (A) *TRPA1*, (B) *TRPV1*, and (C) *IL8* mRNA expression in HBEC3-KT cells following 4- or 12-h treatment with media containing 0.2% DMSO or the PKC activator and the TRPV1 sensitizer PMA. Data (Rq) are the mean ± SD for target gene mRNA expression relative to $\beta 2M$ mRNA and the control ($n = 3$). $^{***}p < 0.001$ and $^{****}p < 0.0001$ using two-way ANOVA and Dunnett's multiple comparison test comparing to the 4 and 12 h gene-specific control. (D) Effects of 12-h treatment with the PKC inhibitor Go6983 (10 μM) and p38 MAPK inhibitor PD169316 (10 μM) on *TRPA1* mRNA expression in HBEC3-KT and SAECs compared with cells treated with media containing 0.2% DMSO. Data (Rq) are the mean ± SD for target gene mRNA expression relative to $\beta 2M$ mRNA and the control. $^{****}p < 0.0001$ using multiple *t*-tests comparing treatment vs. the respective cell type–specific control. (E) *TRPV1* and *IL8* mRNA expression in HBEC3-KT cells following 12-h treatment with media containing 0.2% DMSO or Go6983 (10 μM). $^{*}p \leq 0.05$ and $^{****}p < 0.0001$ using two-way ANOVA and Bonferroni's multiple comparisons test to compare the gene-specific control and treatment group. (F) TRPV1-mediated calcium flux in HEK-293 cells stably overexpressing human TRPV1 with and without 12-h treatment with media containing 0.2% DMSO or the PKC inhibitor Go6983 (10 μM). Data are the mean ± SD for change in fluorescence relative to media-treated cells normalized to the maximum response (100%) and fit using the log [agonist] vs. normalized response-variable slope equation ($n = 3$). $^{**}p < 0.01$ and $^{****}p < 0.0001$ using two-way ANOVA and a Bonferroni test. Raw data are graphed in Figure S8. Summary data can be found in Excel Table S10 (A–C) and Excel Table S11 (D–F). Note: ANOVA, analysis of variance; DMSO, dimethyl sulfoxide; HBEC3-KT, telomerase reverse transcriptase and CDK4–immortalized normal human bronchial epithelial (cells); IL8, interleukin-8; p38 MAPK, p38 mitogen-activated protein kinase; PD169316, a p38 MAPK inhibitor; PKC, protein kinase C; PMA, phorbol 12-myristate 13-acetate; Rq, relative quantification; SAECs, small airway epithelial cells; SD, standard deviation; TRPA1, transient receptor potential cation channel subfamily A member 1; TRPV1, transient receptor potential cation channel subfamily V member 1; $\beta 2M$, β2-microglobulin.

Consistent with a role for PKC and p38 MAPK activity in modulating NF-κB signaling, AECs treated for 12 h with the PKC inhibitor Go6983 and the p38 MAPK inhibitor PD169316 also had lower *TRPA1* mRNA expression: 3.3- ($p < 0.0001$) and 2.9-fold ($p < 0.0001$), respectively (Figure 7D), while simultaneously having 1.4-fold and 2.2-fold higher *TRPV1* ($p = 0.0331$) and *IL8* ($p < 0.0001$) mRNA expression (Figure 7E). Finally, it is possible that the increase in *TRPV1* mRNA expression associated with protracted PKC inhibition in nonstimulated cells by Go6983 (Figure 7E) was driven in part by a reduction in basal TRPV1 activity given that 12-h Go6983 treatment attenuated nonivamide-induced TRPV1 activation in TRPV1-overexpressing HEK-293 cells (Figure 7F). This effect was characterized by a shift in the 50% effective concentration (EC_{50}) from 0.94 ± 0.05 to 2.13 ± 0.04 μM and a decrease in the Hill slope from 2.6 ± 0.3 to 1.1 ± 0.1 (raw data are shown in Figure S8).

Relationship between NF-κB, NLRP2, TRPA1, TRPV1, *and* IL8 *mRNA Expression*

Treatment of HBEC3-KT cells with the NF-κB pathway inhibitor BMS-345541 resulted in ∼5-fold ($p < 0.0001$) lower *NLRP2* mRNA expression (Figure 8A). The role for NLRP2 in *TRPA1* mRNA expression was further evaluated. HBEC3-KT cells transfected with *NLRP2* siRNA-1 and -2 exhibited 1.7 ($p = 0.0078$) and 2.2-fold ($p = 0.005$) lower NLRP2 protein compared with the scramble siRNA control (Figure 8B,C) and 2.7-fold ($p = 0.0001$; Figure 8D) lower *NLRP2* mRNA (*NLRP2* siRNA-2 shown). Unprocessed western blot images for NLRP2 are shown in Figure S9. Finally, cells transfected with *NLRP2* siRNA-2 had 7.4-fold ($p = 0.0077$) higher *TRPA1* (Figure 8E), 2-fold higher *TRPV1* ($p < 0.001$), and 4.3-fold higher ($p = 0.0006$) *IL8* mRNA (Figure 8G). Cells treated with *TRPV1* siRNA also had ∼29-fold ($p < 0.0001$) higher IL8 mRNA (Figure 8H), supporting a role for NLRP2 in regulating the NF-κB-dependent expression of TRPA1 and IL8 and the suppression of TRPV1.

TRPV1 *I585I/V Genotype and Responses of NHBE Cells to PM* in Vitro

NHBE cells from multiple donors (Figure 1B–D) were treated with DEP and CFA. *DDIT3* mRNA expression was used as a biomarker for TRPA1 activation and pathological endoplasmic reticulum stress,[25] and *IL8* mRNA as a marker of inflammation and likely NF-κB activity.[29,40] Both DEP and CFA treatment resulted in higher *IL8* and *DDIT3* mRNA expression relative to the respective untreated donor line control (Figure 9A,B,D,E). In addition, the average fold difference in *DDIT3* and *IL8* mRNA was

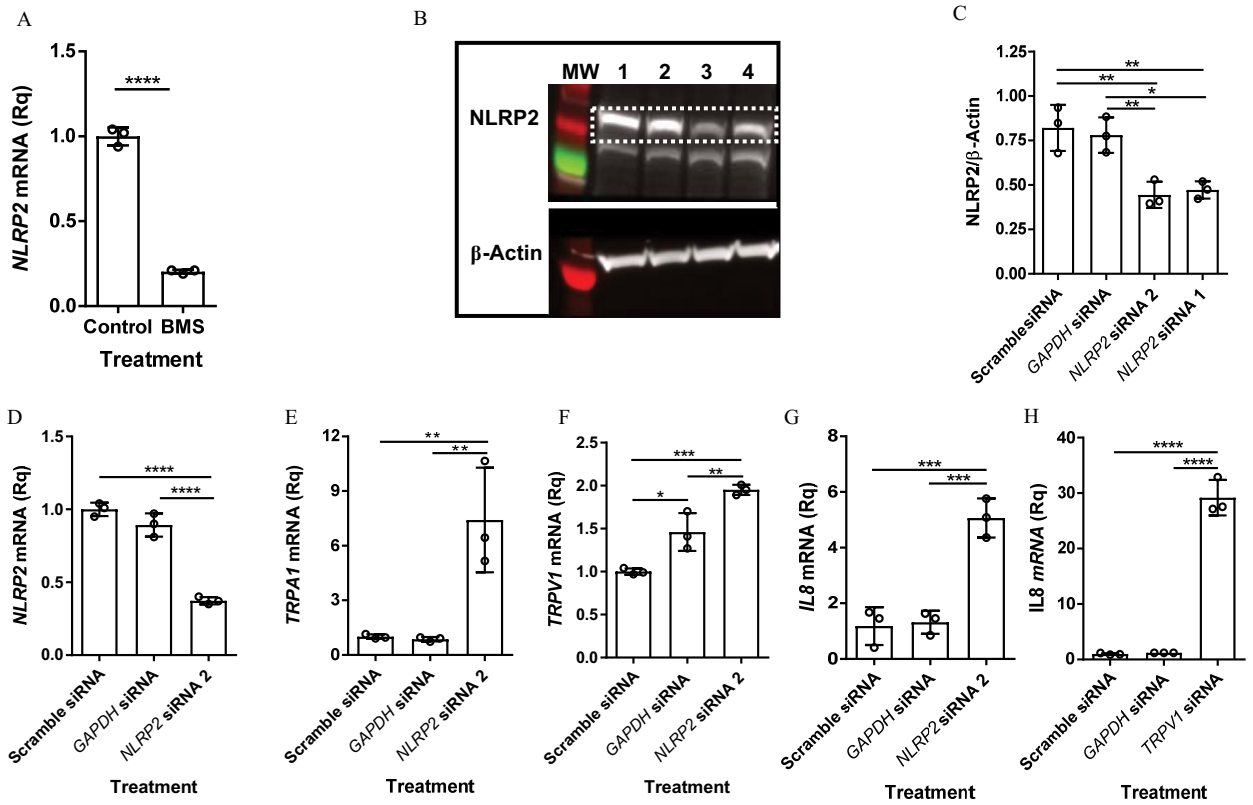

Figure 8. (A) *NLRP2* mRNA expression in HBEC3-KT cells following 24-h treatment with media containing 0.2% DMSO or the NF-κB inhibitor BMS-345541 (10 μM). Data (Rq) are the mean ± SD for target gene mRNA expression relative to *β2M* mRNA and the control ($n=3$). $^{****}p<0.0001$ using a one-tailed, unpaired Student's *t*-test. (B) Representative western blot image for NLRP2 in HBEC3-KT cells transfected with 100 pmol/mL *NLRP2* siRNA, where, from left to right, are the molecular weight standards (MW), scramble siRNA (1), *GAPDH* siRNA (2), and *NLRP2* siRNA 1 and 2 transfected cell lysates (3 and 4). (C) Quantification of NLRP2 protein in siRNA-transfected HBEC3-KTs. Raw data are provided in Figure S9. Data are the mean ± SD of the ratio of NLRP2 to β-actin band density ($n=3$). $^{*}p\leq0.05$ and $^{**}p<0.01$ using one-way ANOVA and Tukey's multiple comparison test comparing all groups. (D–G) *NLRP2*, *TRPA1*, *TRPV1*, and *IL8* mRNA expression in HBEC3-KTs 24 h after *NLRP2* siRNA-2 (100 pmol) transfection, and (H) *IL8* mRNA expression following *TRPV1* siRNA (500 pmol) transfection compared with the respective control siRNA and *GAPDH* siRNA groups. Data (Rq) are the mean ± SD for target gene mRNA expression relative to *β2M* mRNA and the scramble control ($n=3$). $^{**}p<0.01$, $^{***}p<0.001$, and $^{****}p<0.0001$ using one-way ANOVA and Tukey's multiple comparison test comparing all groups. Summary data can be found in Excel Table S12. Note: ANOVA, analysis of variance; BMS, BMS-345541; DMSO, dimethyl sulfoxide; GAPDH, glyceraldehyde 3-phosphate dehydrogenase; HBEC3-KT, telomerase reverse transcriptase and CDK4–immortalized normal human bronchial epithelial (cells); IL8, interleukin-8; NF-κB, nuclear factor kappa light chain enhancer of activated B cells; NLRP2, nucleotide-binding oligomerization domain, leucine rich repeat and pyrin domain containing 2; Rq, relative quantification; SD, standard deviation; siRNA, small interfering RNA; TRPA1, transient receptor potential cation channel subfamily A member 1; TRPV1, transient receptor potential cation channel subfamily V member 1; *β2M*, β2-microglobulin.

greater for cells with the I585I/V genotype: 2.3-fold ($p=0.0047$) for DEP and 3.6-fold ($p=0.2123$) for CFA (Figure 9C). For *IL8*, responses were also greater in I585I/V expressing cells, but not significant ($p=0.285$ and 0.2029, respectively for DEP and CFA; Figure 9F). Correlation analysis confirmed an association between *TRPV1* I585I/V genotype and *TRPA1* mRNA expression (0.54), as well as for DEP-induced *DDIT3* mRNA expression (0.93; Figure S10). A negative correlation between *TRPV1* mRNA expression and the I585I/V genotype (−0.34) was also observed. Finally, stratification of the *DDIT3* and *IL8* mRNA expression data as a function of either the *TRPV1* I315M (Figure S11) or T469I (Figure S12) genotypes did not show evidence of an effect on *in vitro* cellular responses to DEP or CFA.

Gain and Loss-of-Function TRPA1 *and* TRPV1 *SNPs and Asthma Symptom Control as a Function of Cigarette Smoke Exposure*

Stratifying asthma control data for *TRPV1* I585V allele expression and tobacco smoke exposure among children with asthma revealed worse asthma control for the I585I/I+V/V genotype combination with smoke exposure ($p=0.0346$; Figure 10A). In fact, an unexpected trend toward improved control for the I585I/V genotype was observed for smoke exposure. In addition, the essentially co-inherited *TRPA1* R3C and R58T SNPs,[26] or ≥1 allelic copy of the *TRPV1* I315M or T469I SNPs were associated with poorer symptom control ($p=0.0684$, 0.0143, and 0.0031, respectively; Figure 10B–D) compared with individuals of the same genotype without smoke exposure. For comparison, the effects of several other SNPs previously reported to be associated with asthma risk or asthma symptoms associated with tobacco smoke including rs1871042 and rs6591255 (glutathione *S*-transferase pi 1),[55,56] rs4073 (IL8),[57] rs1800925 (IL13),[58,59] rs1042713 (adrenergic receptor beta-1),[60] and rs2243250 (IL4)[61] were also evaluated (Figure S13). In all cases, tobacco smoke exposure was associated with worse asthma symptom control, having similar effect sizes as the *TRPA1* and *TRPV1* SNPs, but genotype-specific associations were not observed as they were for the TRP SNPs.

Discussion

From 2020 data, the Centers for Disease Control and Prevention estimates that >25 million people in the United States have asthma.[62] Literature shows that exposure to environmental

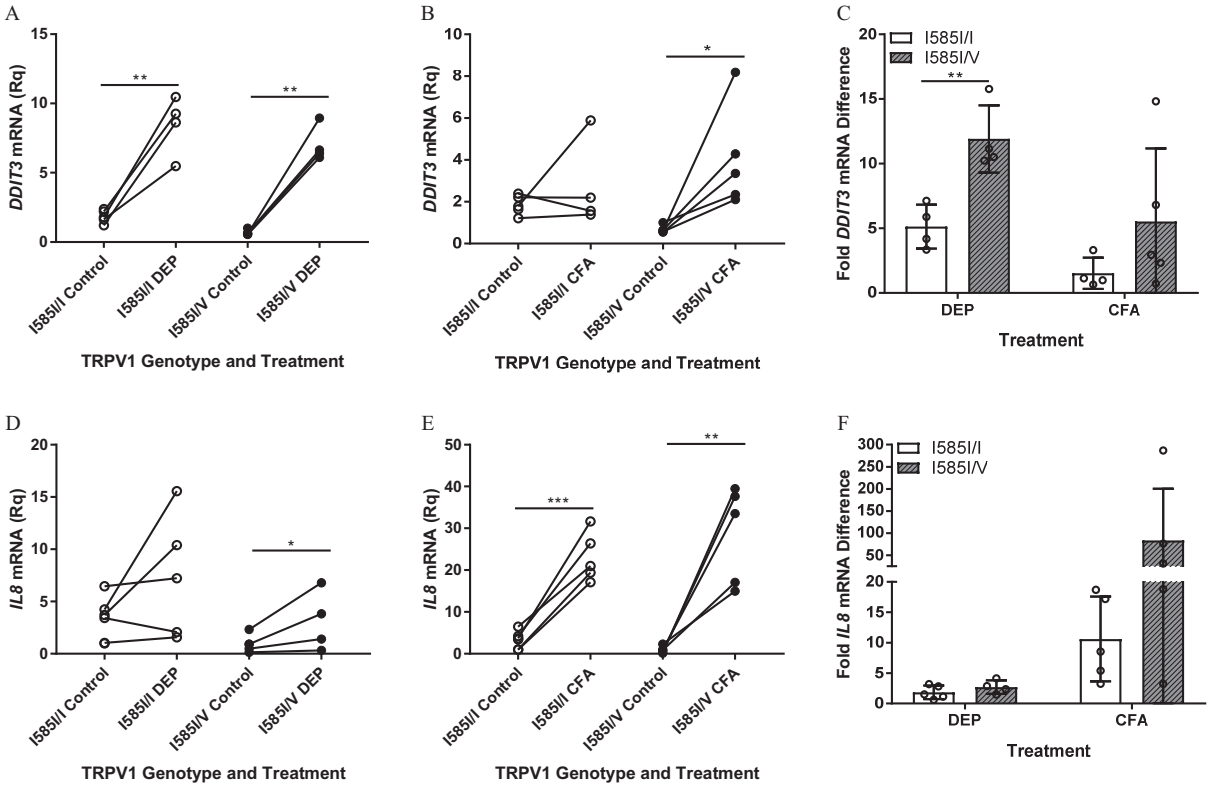

Figure 9. (A–C) *DDIT3* and (D–F) *IL8* mRNA expression in NHBE cells having either the *TRPV1* I585I/I or I585I/V genotype 24 h after treatment with media containing either 0.2% DMSO, DEP (CFA 10 $\mu g/cm^2$), or CFA (180 $\mu g/cm^2$) treatment ($n \geq 4$ donors/genotype). (A,B,D,E) Data (Rq) are the mean ± SD for target gene mRNA expression normalized to *β2M* mRNA, analyzed using a paired one-tailed *t*-test. Fold change in (C) *DDIT3* and (F) *IL8* mRNA expression in DEP- and CFA-treated cells normalized to media-treated controls for each donor. $^{*}p \leq 0.05$ using multiple *t*-tests to compare genotype effects for each particle. Summary data can be found in Excel Table S13. Note: CFA, coal fly ash; DDIT3, DNA damage-inducible transcript-3; DEP, diesel exhaust particles; DMSO, dimethyl sulfoxide; IL8, interleukin-8; NHBE, normal human bronchial epithelial (cells); Rq, relative quantification; SD, standard deviation; TRPV1, transient receptor potential cation channel subfamily V member 1; *β2M*, β2-microglobulin.

pollution increases risks for developing asthma among children and that asthmatics are more susceptible to exacerbation by environmental pollutants.[7–13] Previous *in vitro* studies by our group have demonstrated that both TRPA1 and TRPV1 were variably activated by captured PM, including WSPM,[24,25] DEP,[4,5] CFA[3,15] and cigarette smoke PM (CSPM)[6]. Depending upon source and composition, WSPM, DEP, and CSPM can be potent TRPA1 agonists, whereas CFA was shown to be a weak TRPA1 agonist,[26] as well as an agonist of both TRPV1[3,15] and TRPM8.[3,34] Because both TRPA1 and TRPV1 are implicated in the pathogenesis of asthma, this study tested the hypothesis that differences in TRPA1 expression and activity as a function of TRPV1 genetics may contribute to variations in AEC responses to PM challenge *in vitro* and asthma control, particularly as a function of one's environmental exposure profile (i.e., their exposome or envirome), via altered sensitivity of AECs to PM and TRPA1 agonists.

The first objective of this study was to determine the mechanism driving higher TRPA1 expression by AECs having the *TRPV1* I585I/V genotype. *In vitro* results suggest an integrated network consisting of PKC, p38 MAPK, NF-κB, and NLRP2 in regulating basal and dynamic TRPA1 expression in AECs. The activity of this network was *TRPV1*-genotype and -activity dependent, and TRPA1 activation itself served as a catalyst for variable expression. Multiple endogenous proinflammatory stimuli that directly or indirectly activate NF-κB (e.g., TNFα, IL1α, IL1β) and orchestrate pulmonary inflammation, also affected TRPA1 expression. A hypothetical mechanism for how the *TRPV1* genotype and associated changes in basal activity affect TRPA1 expression is presented in Figure 11. Further, the role of TRPA1 activation as a trigger for dynamic expression of TRPA1 and other TRPs (e.g., TRPV3) is shown in Figure 12.

The role of NF-κB in regulating TRPA1 expression has previously been shown in keratinocytes,[63] A549 cells,[64] and synoviocytes.[63–66] The present study identified a comparable mechanism regulating basal and dynamic TRPA1 expression in AECs and further identified a relationship wherein loss or attenuation expression and function paradoxically promoted TRPA1 expression and function. Conversely, when TRPV1 was activated or more abundant, TRPA1 expression/function was lower. This relationship was also reciprocal in that TRPA1 activation using multiple agonists, including WSPM and AITC, led to transiently higher levels of *TRPV1* mRNA and lower *TRPA1* mRNA relative to control cells. Regarding this paradigm, the *TRPV1* I585I/V genotype of HBEC3-KT cells was likely paramount, although dynamic expression of TRPA1 (and other TRPs) in BEAS-2B and NHBE AECs with the *TRPV1* I585I/I genotype was/has also been observed.[15,25,31] Regardless, this connection between TRP channels and TRP channel agonists is likely to have important consequences with respect to AEC and individual sensitivity to specific environmental stimuli and asthma triggers, as well as the ability to therapeutically manipulate TRPA1 or TRPV1 for pain, inflammation, and other purposes. Accordingly, a general recommendation is that this relationship be considered when studying TRPA1 and TRPV1 in AECs and possibly other cell types, particularly when evaluating the effects of pollutants or chemicals that may target one or both receptors.

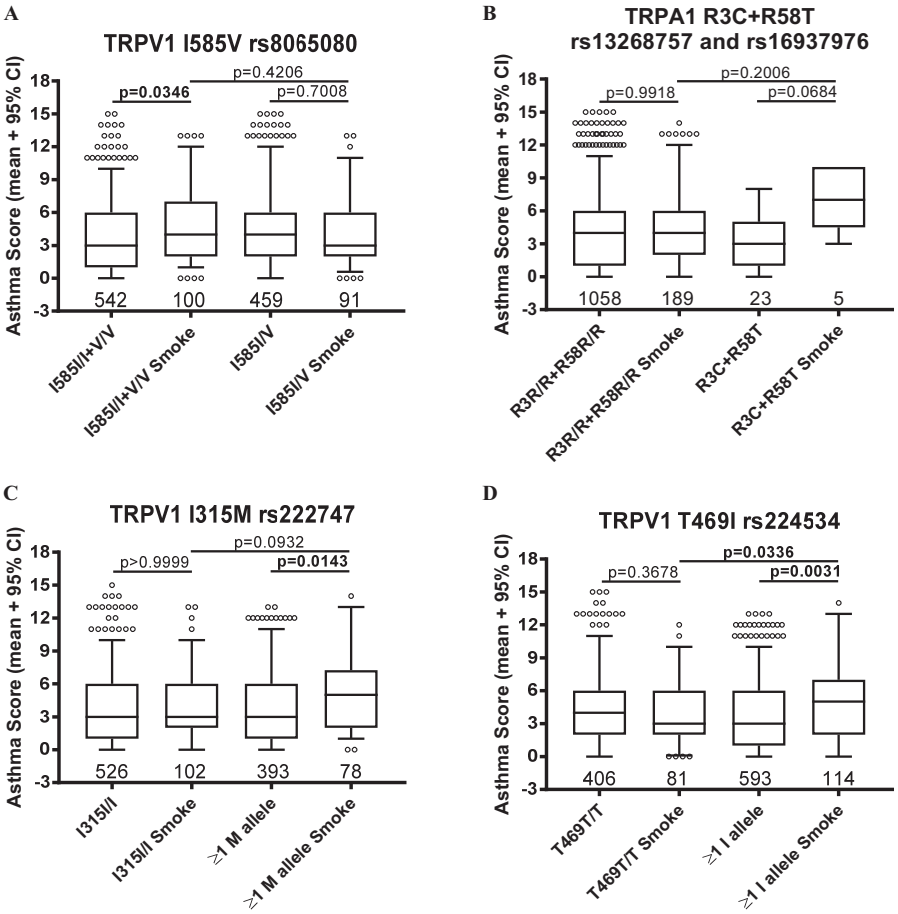

Figure 10. Average asthma control score as a function of (A) *TRPV1* I585V, (B) *TRPA1* R3C/R58T, (C) *TRPV1* I315M, and (D) *TRPV1* T469I genotype and as a function of voluntarily reported tobacco smoke exposure. Data are the means ± 95% confidence intervals (CIs) using one-way ANOVA and Bonferroni's multiple comparison test. Subject numbers and *p*-values are shown. Summary data can be found in Excel Table S16. Note: ANOVA, analysis of variance; TRPA1, transient receptor potential cation channel subfamily A member 1; TRPV1, transient receptor potential cation channel subfamily V member 1.

A key aspect of TRPA1 regulation seemingly involved basal and temporal differences in NF-κB activity and associated NLRP2 expression as a function of cell status. In *TRPV1* I585I/I cells, the markedly higher levels basal *NLRP2* and *IGFBP2* expression could suggest a higher level of basal NF-κB activity. Although not proven, it is tempting to hypothesize that higher *NLRP2* and *IGFBP2* expression may represent a mechanism to control basal inflammation mediated by NF-κB and TRPV1. Specifically, higher/more active TRPV1 could promote NF-κB signaling and increased *IL8*, *NLRP2*, and *IGFBP2* expression, leading to the suppression of *TRPA1* and cellular effects associated with changes in TRPA1 activity. Conversely, lower expression of *NLRP2* in TRPV1 I585I/V cells could reflect a basally suppressed inflammatory state, due to less active TRPV1, and less need to negatively suppress NF-κB–regulated genes by NLRP2 feedback inhibition,[41,42] including IL8 and TRPA1. Of significance, multiple TRP and pro-inflammatory stimuli that promote NF-κB signaling impacted this network, including TNFα, IL1α/β, and modifiers of PKC and p38 MAPK. PKC activation is regulated by intracellular calcium, which is a likely consequence of variable TRP activity. Here, activating PKC by PMA,[53,54] which would also promote TRPV1 activity[53,54] and NF-κB signaling led to a rapid but diminishing increase in *IL8* and *TRPV1* expression, as well as a delayed reduction in *TRPA1* expression. This likely occurred by short term stimulation of NF-κB-driven transcription, followed by a period of attenuated activity due to NLRP2-dependent negative feedback on NF-κB.[41,42] Interestingly, inhibiting both PKC and p38 MAPK, which would attenuate basal NF-κB activity, also resulted in lower *TRPA1* mRNA expression and higher *TRPV1* expression, collectively demonstrating that the balance of NF-κB activation and the expression of NF-κB–regulated genes, including *NLRP2*, determined the TRPA1/TRPV1/IL8 dynamic. More work is necessary to validate and fully unravel the scope of interactions involved in the control of TRPA1 and TRPV1 expression/function by PKC, p38 MAPK, and presumably other kinases/phosphatases, and specifically how NRLP2 and NF-κB activities are altered. Such work should also address the limitation of this work by defining the kinetics of these interactions at the protein/activity level. Regardless, the finding that these entities communicated to affect TRP activity and expression basally and during inflammation/cell damage provides key insights into the complex, but orchestrated, regulation of TRP signaling during basal and pathological states, including following exposure of AECs to potential asthma triggers. Given the vital role of NF-κB in regulating pulmonary homeostasis, it is reasonable to conclude that the balance of this mechanistic hub may also play a key role in shaping cellular responses to various pro-inflammatory agents relevant to asthma.

A second objective of this study was to determine whether the I585I/V genotype and elevated TRPA1 expression would be consequential with respect to the effects of environmental pollutants

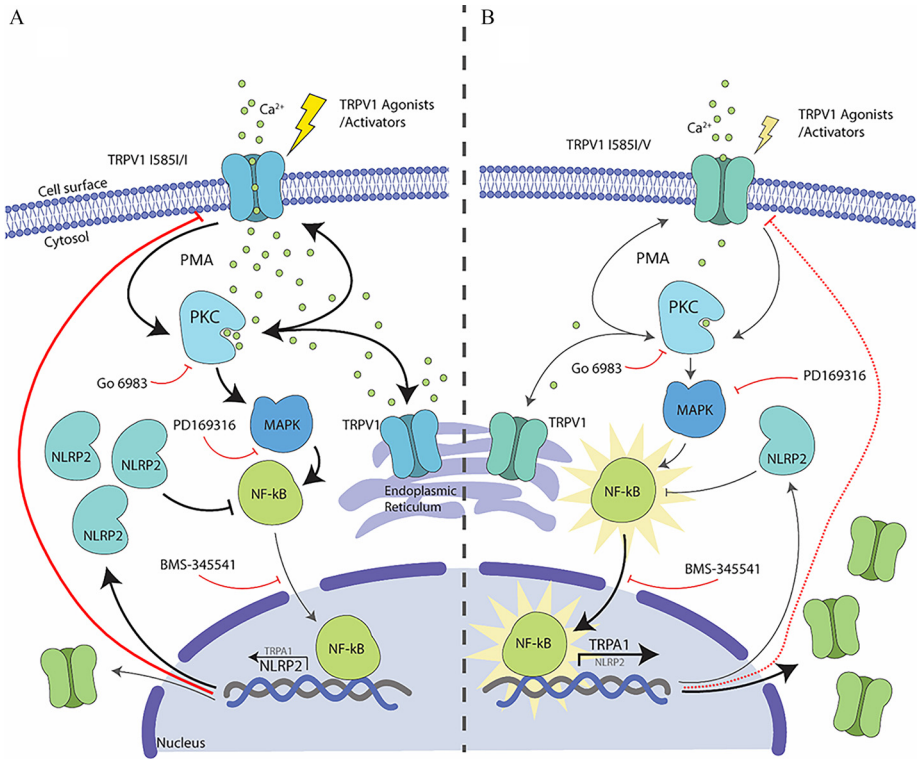

Figure 11. Schematic summarizing the authors hypothesis for how TRPV1, NF-κB, PKC, and p38 MAPK may regulate TRPA1, TRPV1, and NLRP2 expression in AECs. The summary is based on the cumulative results of this and other referenced studies. (A) TRPV1 I585I/I and (B) TRPV1 I585I/V. Note: AECs, airway epithelial cells; Ca^{2+}, calcium ions; Go6983, a PKC inhibitor; NF-κB, nuclear factor kappa light chain enhancer of activated B cells; NLRP2, nucleotide-binding oligomerization domain, leucine rich repeat and pyrin domain containing 2; MAPK, p38 mitogen-activated protein kinase; PD169316, a p38 MAPK inhibitor; PKC, protein kinase C; PMA, phorbol 12-myristate 13-acetate; TRPA1, transient receptor potential cation channel subfamily A member 1; TRPV1, transient receptor potential cation channel subfamily V member 1.

on AECs *in vitro* and, ultimately, on asthma control. A theme that was consistent throughout this study was the inverse relationship between *TRPA1* and *TRPV1* mRNA expression and activity. The discovery of this balance, and the degree to which it is influenced by multiple *TRPV1* genotypes and TRPA1 and TRPV1 agonists is unique, intriguing, and seemingly indicative of a broad mechanism for regulating inflammation and general cellular homeostasis in which TRPA1 and TRPV1 may play different, but defined roles in a context-dependent manner. Specifically, cellular calcium homeostasis is critical, with acute and chronic perturbations serving as a catalyst for many effects of stimuli, including those driven by PKC, p38 MAPK, and NF-κB. Results here suggest that regulation of an intracellular calciome is in part dependent upon TRPA1, TRPV1, and other dynamically regulated TRPs such as TRPV3, which seemingly act in concert to shape how cells respond to TRPA1 agonists, environmental stimuli, and even endogenous pro-inflammatory mediators relevant to asthma and airway physiology/pathophysiology in general. This conceptual framework is supported by both our prior work demonstrating the modulation of TRPA1, endoplasmic reticulum stress, and growth/repair in HBEC3-KT and other AECs by TRPV3,[25,31] as well as by findings here that TRP genetics, and changes in TRPA1 and TRPV1 expression and function affect acute cellular responses to PM *in vitro* and asthma control as a function of tobacco smoke exposure.

Regarding the consequences of variable TRPA1 or TRPV1 expression/function on asthma control, results from a cohort analysis did not support the hypothesized association between the *TRPV1* I585I/V genotype and worse asthma control as a function of smoke exposure. Rather, an unexpected trend indicative of better symptom control for individuals with the I585I/V genotype was observed, opposite that of individuals with the I585I/I+I585V/V and other *TRPA1* and *TRPV1* genotypes evaluated. Despite limitations related to the use of self- and parental/guardian-reported smoke exposure (i.e., exposure is likely underreported), and the levels of expression/activity of the TRPs and other elements of the proposed regulatory network were not evaluated, several findings suggest the observed genotype–phenotype trends could be clinically relevant. First, higher TRPA1 expression and activity associated with the *TRPV1* I585I/V genotype and tobacco smoke exposure would be expected to promote calcium-dependent PKC activation,[67] acute sensitization of TRPV1,[53,54,67] and TRPA1 suppression. With time, protracted PKC activation could also desensitize TRPV1. Second, despite the possibility that TRPV1 may become induced by TRPA1 agonists, at least with acute exposures, loss of function associated with *TRPV1* I585V expression may render this effect irrelevant, whereas higher levels of expression of more active TRPV1 I315M and T469I[15] may sensitize asthmatics to a broader array of stimuli, including non-TRPA1 agonists. This could explain why the *TRPV1* I585V/V genotype has previously been associated with improved asthma symptom control[15,27,28] and why the I315M and T469M genotypes have been associated with poorer symptom control with smoking. Interestingly, the effects of several other SNPs previously reported to be associated with asthma risk or asthma symptoms also showed associations with tobacco smoke exposure, but genotype-specific associations with asthma control were not observed, suggesting unique effects of TRP SNPs in regulating asthma control.

Finally, a person's individual exposures must be considered with respect to the mechanisms described herein, and in understanding discrepancies between the *in vitro* observations related to the TRPA1/TRPV1 dynamic and asthma control. Specifically, the *in vitro* studies provide insight into how potential asthma-exacerbating stimuli could acutely perturb the NF-κB/TRP/IL8

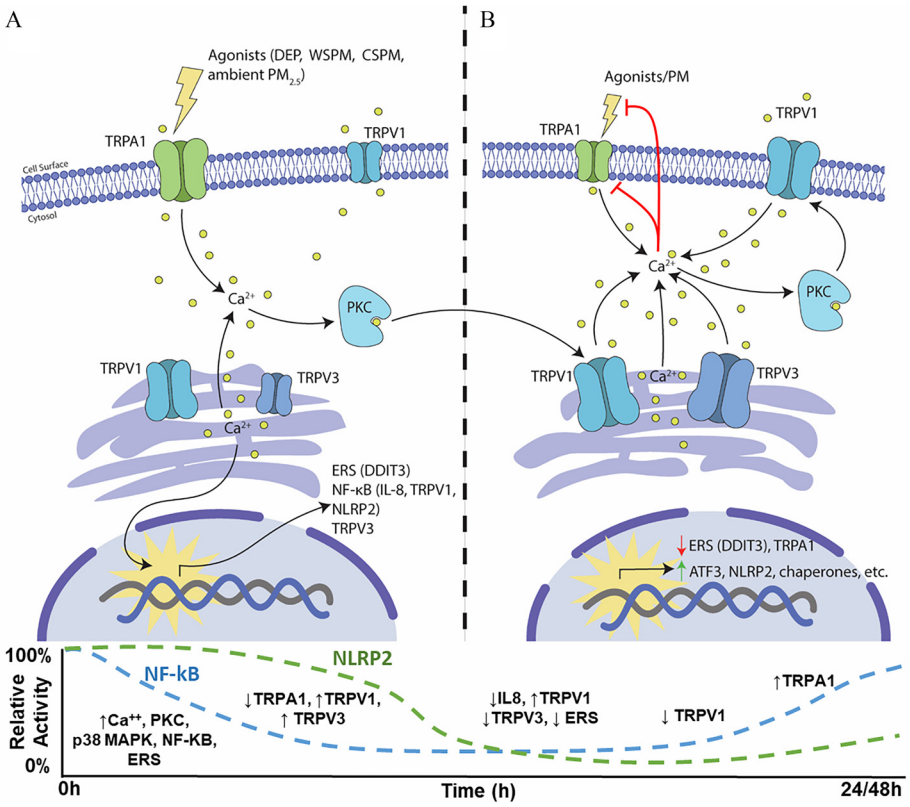

Figure 12. Schematic summarizing the authors hypothesis for how TRPA1 activation may affect the expression/function of TRPs involved in calcium handling (TRPV1 and TRPV3 shown) and cytotoxic ERS, thus modulating responses to TRPA1 stimuli. The summary is based on the cumulative results of this and other referenced studies. (A) No TRPA1 activation; (B) TRPA1 activation. A timeline representing the relative activities of NF-κB and NLRP2 following TRPA1 stimulation is also shown. Western blot and mRNA expression data supporting this timeline are shown in Figure S14. Note: ATF3, activating transcription factor 3; Ca^{2+}, calcium ions; CSPM, cigarette smoke particulate matter; DDIT3, DNA damage-inducible transcript-3; DEP, diesel exhaust particles; ERS, endoplasmic reticulum stress; IL8, interleukin-8; NF-κB, nuclear factor kappa light chain enhancer of activated B cells; NLRP2, nucleotide-binding oligomerization domain, leucine rich repeat and pyrin domain containing 2; PKC, protein kinase C; PM, particulate material; $PM_{2.5}$, particulate matter ≤ 2.5 μm in aerodynamic diameter; TRP, transient receptor potential; TRPA1, transient receptor potential cation channel subfamily A member 1; TRPV1, transient receptor potential cation channel subfamily V member 1; TRPV3, transient receptor potential cation channel subfamily V member 3; WSPM, wood smoke particulate matter.

balance, which may be more applicable to people who are not regularly exposed to TRPA1 agonists such as tobacco smoke but then are subsequently exposed. Alternatively, the cohort data provides insights on how chronic exposure to tobacco smoke (or perhaps other pollutants/TRPA1 agonists) may impact this dynamic; specifically, that TRPA1 signaling may become suppressed, whereas TRPV1 may become amplified.

To summarize, asthma symptom control is the product of an individual's genetics, responses to therapeutics, medication adherence, lifestyle (diet and exercise), infection status, and exposure to indoor and outdoor triggers. Air pollutants can promote and exacerbate existing asthma by activating *TRPA1* and *TRPV1*. A mechanism was demonstrated by which *TRPV1* genotype and TRPV1 activity, as well as activation of *TRPA1* itself, influenced TRPA1, TRPV1, other TRP expression by AECs through NF-κB signaling. Further, it was shown that the balance of TRPA1 and TRPV1 expression and activity was consequential in that higher TRPA1 expression was associated with higher acute cellular responses to selected model pollutants *in vitro* in AECs with the I585I/V genotype. However, analysis of asthma cohort data indicated a more complex relationship between TRPA1 and TRPV1, likely driven by variations in exposure to distinct types of asthma triggers. Overall, this study provides early but intriguing insight into how the *TRPV1* I585I/V genotype and other SNPs, variable TRP expression, and exposure to certain types of pollutants may coordinately affect *in vitro* cellular responses to pollutant challenges and a person's asthma in a variable environment.

Acknowledgments

This work was supported by the National Institutes of Health/National Institute of Environmental Health Sciences [grants ES017431 and ES027015 (to C.A.R.)] and National Institute of General Medical Sciences [grant GM121648 (to C.A.R.)].

References

1. Basbaum AI, Bautista DM, Scherrer G, Julius D. 2009. Cellular and molecular mechanisms of pain. Cell 139(2):267–284, PMID: 19837031, https://doi.org/10.1016/j.cell.2009.09.028.
2. Julius D. 2013. TRP channels and pain. Annu Rev Cell Dev Biol 29:355–384, PMID: 24099085, https://doi.org/10.1146/annurev-cellbio-101011-155833.
3. Deering-Rice CE, Johansen ME, Roberts JK, Thomas KC, Romero EG, Lee J, et al. 2012. Transient receptor potential vanilloid-1 (TRPV1) is a mediator of lung toxicity for coal fly ash particulate material. Mol Pharmacol 81(3):411–419, PMID: 22155782, https://doi.org/10.1124/mol.111.076067.
4. Deering-Rice CE, Memon T, Lu Z, Romero EG, Cox J, Taylor-Clark T, et al. 2019. Differential activation of TRPA1 by diesel exhaust particles: relationships between chemical composition, potency, and lung toxicity. Chem Res Toxicol 32(6):1040–1050, PMID: 30945539, https://doi.org/10.1021/acs.chemrestox.8b00375.
5. Deering-Rice CE, Romero EG, Shapiro D, Hughen RW, Light AR, Yost GS, et al. 2011. Electrophilic components of diesel exhaust particles (DEP) activate

transient receptor potential ankyrin-1 (TRPA1): a probable mechanism of acute pulmonary toxicity for DEP. Chem Res Toxicol 24(6):950–959, PMID: 21591660, https://doi.org/10.1021/tx200123z.
6. Shapiro D, Deering-Rice CE, Romero EG, Hughen RW, Light AR, Veranth JM, et al. 2013. Activation of transient receptor potential ankyrin-1 (TRPA1) in lung cells by wood smoke particulate material. Chem Res Toxicol 26(5):750–758, PMID: 23541125, https://doi.org/10.1021/tx400024h.
7. Tuazon JA, Kilburg-Basnyat B, Oldfield LM, Wiscovitch-Russo R, Dunigan-Russell K, Fedulov AV, et al. 2022. Emerging insights into the impact of air pollution on immune-mediated asthma pathogenesis. Curr Allergy Asthma Rep 22(7):77–92, PMID: 35394608, https://doi.org/10.1007/s11882-022-01034-1.
8. Grant TL, Wood RA. 2022. The influence of urban exposures and residence on childhood asthma. Pediatr Allergy Immunol 33(5):e13784, PMID: 35616896, https://doi.org/10.1111/pai.13784.
9. Chen Z, Salam MT, Eckel SP, Breton CV, Gilliland FD. 2015. Chronic effects of air pollution on respiratory health in Southern California children: findings from the Southern California Children's Health Study. J Thorac Dis 7(1):46–58, PMID: 25694817, https://doi.org/10.3978/j.issn.2072-1439.2014.12.20.
10. Madaniyazi L, Xerxes S. 2021. Outdoor air pollution and the onset and exacerbation of asthma. Chronic Dis Transl Med 7(2):100–106, PMID: 34136769, https://doi.org/10.1016/j.cdtm.2021.04.003.
11. Orellano P, Quaranta N, Reynoso J, Balbi B, Vasquez J. 2017. Effect of outdoor air pollution on asthma exacerbations in children and adults: systematic review and multilevel meta-analysis. PLoS One 12(3):e0174050, PMID: 28319180, https://doi.org/10.1371/journal.pone.0174050.
12. Orellano P, Quaranta N, Reynoso J, Balbi B, Vasquez J. 2018. Association of outdoor air pollution with the prevalence of asthma in children of Latin America and the Caribbean: a systematic review and meta-analysis. J Asthma 55(11):1174–1186, PMID: 29211546, https://doi.org/10.1080/02770903.2017.1402342.
13. Thurston GD, Balmes JR, Garcia E, Gilliland FD, Rice MB, Schikowski T, et al. 2020. Outdoor air pollution and new-onset airway disease. An official American Thoracic Society workshop report. Ann Am Thorac Soc 17(4):387–398, PMID: 32233861, https://doi.org/10.1513/AnnalsATS.202001-046ST.
14. Andrade EL, Meotti FC, Calixto JB. 2012. TRPA1 antagonists as potential analgesic drugs. Pharmacol Ther 133(2):189–204, PMID: 22119554, https://doi.org/10.1016/j.pharmthera.2011.10.008.
15. Deering-Rice CE, Stockmann C, Romero EG, Lu Z, Shapiro D, Stone BL, et al. 2016. Characterization of transient receptor potential vanilloid-1 (TRPV1) variant activation by coal fly ash particles and associations with altered transient receptor potential ankyrin-1 (TRPA1) expression and asthma. J Biol Chem 291(48):24866–24879, PMID: 27758864, https://doi.org/10.1074/jbc.M116.746156.
16. Jordt SE. 2021. TRPA1: an asthma target with a zing. J Exp Med 218(4):e20202507, PMID: 33625497, https://doi.org/10.1084/jem.20202507.
17. Bessac BF, Jordt SE. 2008. Breathtaking TRP channels: TRPA1 and TRPV1 in airway chemosensation and reflex control. Physiology (Bethesda) 23:360–370, PMID: 19074743, https://doi.org/10.1152/physiol.00026.2008.
18. Long L, Yao H, Tian J, Luo W, Yu X, Yi F, et al. 2019. Heterogeneity of cough hypersensitivity mediated by TRPV1 and TRPA1 in patients with chronic refractory cough. Respir Res 20(1):112, PMID: 31170994, https://doi.org/10.1186/s12931-019-1077-z.
19. Groneberg DA, Niimi A, Dinh QT, Cosio B, Hew M, Fischer A, et al. 2004. Increased expression of transient receptor potential vanilloid-1 in airway nerves of chronic cough. Am J Respir Crit Care Med 170(12):1276–1280, PMID: 15447941, https://doi.org/10.1164/rccm.200402-174OC.
20. McGarvey LP, Butler CA, Stokesberry S, Polley L, McQuaid S, Abdullah H, et al. 2014. Increased expression of bronchial epithelial transient receptor potential vanilloid 1 channels in patients with severe asthma. J Allergy Clin Immunol 133(3):704–712.e4, PMID: 24210884, https://doi.org/10.1016/j.jaci.2013.09.016.
21. Caceres AI, Brackmann M, Elia MD, Bessac BF, del Camino D, D'Amours M, et al. 2009. A sensory neuronal ion channel essential for airway inflammation and hyperreactivity in asthma. Proc Natl Acad Sci USA 106(22):9099–9104, PMID: 19458046, https://doi.org/10.1073/pnas.0900591106.
22. Baker K, Raemdonck K, Dekkak B, Snelgrove RJ, Ford J, Shala F, et al. 2016. Role of the ion channel, transient receptor potential cation channel subfamily V member 1 (TRPV1), in allergic asthma. Respir Res 17(1):67, PMID: 27255083, https://doi.org/10.1186/s12931-016-0384-x.
23. Song J, Kang J, Lin B, Li J, Zhu Y, Du J, et al. 2017. Mediating role of TRPV1 ion channels in the co-exposure to PM2.5 and formaldehyde of Balb/c mice asthma model. Sci Rep 7(1):11926, PMID: 28931832, https://doi.org/10.1038/s41598-017-11833-6.
24. Memon TA, Nguyen ND, Burrell KL, Scott AF, Almestica-Roberts M, Rapp E, et al. 2020. Wood smoke particles stimulate MUC5AC overproduction by human bronchial epithelial cells through TRPA1 and EGFR signaling. Toxicol Sci 174(2):278–290, PMID: 31944254, https://doi.org/10.1093/toxsci/kfaa006.
25. Nguyen ND, Memon TA, Burrell KL, Almestica-Roberts M, Rapp E, Sun L, et al. 2020. Transient receptor potential ankyrin-1 and vanilloid-3 differentially regulate endoplasmic reticulum stress and cytotoxicity in human lung epithelial cells after pneumotoxic wood smoke particle exposure. Mol Pharmacol 98(5):586–597, PMID: 32938721, https://doi.org/10.1124/molpharm.120.000047.
26. Deering-Rice CE, Shapiro D, Romero EG, Stockmann C, Bevans TS, Phan QM, et al. 2015. Activation of transient receptor potential ankyrin-1 by insoluble particulate material and association with asthma. Am J Respir Cell Mol Biol 53(6):893–901, PMID: 26039217, https://doi.org/10.1165/rcmb.2015-0086OC.
27. Cantero-Recasens G, Gonzalez JR, Fandos C, Duran-Tauleria E, Smit LAM, Kauffmann F, et al. 2010. Loss of function of transient receptor potential vanilloid 1 (TRPV1) genetic variant is associated with lower risk of active childhood asthma. J Biol Chem 285(36):27532–27535, PMID: 20639579, https://doi.org/10.1074/jbc.C110.159491.
28. Sadofsky LR, Cantero-Recasens G, Wright C, Valverde MA, Morice AH. 2017. TRPV1 polymorphisms influence capsaicin cough sensitivity in men. J Thorac Dis 9(3):839–840, PMID: 28449493, https://doi.org/10.21037/jtd.2017.03.50.
29. Reilly CA, Johansen ME, Lanza DL, Lee J, Lim JO, Yost GS. 2005. Calcium-dependent and independent mechanisms of capsaicin receptor (TRPV1)-mediated cytokine production and cell death in human bronchial epithelial cells. J Biochem Mol Toxicol 19(4):266–275, PMID: 16173059, https://doi.org/10.1002/jbt.20084.
30. Deering-Rice CE, Nguyen N, Lu Z, Cox JE, Shapiro D, Romero EG, et al. 2018. Activation of TRPV3 by wood smoke particles and roles in pneumotoxicity. Chem Res Toxicol 31(5):291–301, PMID: 29658714, https://doi.org/10.1021/acs.chemrestox.7b00336.
31. Burrell KL, Nguyen ND, Deering-Rice CE, Memon TA, Almestica-Roberts M, Rapp E, et al. 2021. Dynamic expression of transient receptor potential vanilloid-3 and integrated signaling with growth factor pathways during lung epithelial wound repair following wood smoke particle and other forms of lung cell injury. Mol Pharmacol 100(3):295–307, PMID: 34290137, https://doi.org/10.1124/molpharm.121.000280.
32. Smith KR, Veranth JM, Kodavanti UP, Aust AE, Pinkerton KE. 2006. Acute pulmonary and systemic effects of inhaled coal fly ash in rats: comparison to ambient environmental particles. Toxicol Sci 93(2):390–399, PMID: 16840564, https://doi.org/10.1093/toxsci/kfl062.
33. Cao X, Xu X, Cui W, Xi Z. 2001. Development and certification of a coal fly ash certified reference material for selected polycyclic aromatic hydrocarbons. Fresenius J Anal Chem 370(8):1035–1040, PMID: 11583083, https://doi.org/10.1007/s002160100939.
34. Lamb JG, Romero EG, Lu Z, Marcus SK, Peterson HC, Veranth JM, et al. 2017. Activation of human transient receptor potential melastatin-8 (TRPM8) by calcium-rich particulate materials and effects on human lung cells. Mol Pharmacol 92(6):653–664, PMID: 29038158, https://doi.org/10.1124/mol.117.109959.
35. Reilly CA, Taylor JL, Lanza DL, Carr BA, Crouch DJ, Yost GS. 2003. Capsaicinoids cause inflammation and epithelial cell death through activation of vanilloid receptors. Toxicol Sci 73(1):170–181, PMID: 12721390, https://doi.org/10.1093/toxsci/kfg044.
36. Livak KJ, Schmittgen TD. 2001. Analysis of relative gene expression data using real-time quantitative PCR and the $2^{-\Delta\Delta C(T)}$ method. Methods 25(4):402–408, PMID: 11846609, https://doi.org/10.1006/meth.2001.1262.
37. Schneider CA, Rasband WS, Eliceiri KW. 2012. NIH image to ImageJ: 25 years of image analysis. Nat Methods 9(7):671–675, PMID: 22930834, https://doi.org/10.1038/nmeth.2089.
38. Stockmann C, Fassl B, Gaedigk R, Nkoy F, Uchida DA, Monson S, et al. 2013. Fluticasone propionate pharmacogenetics: CYP3A4*22 polymorphism and pediatric asthma control. J Pediatr 162(6):1222–1227.e2, PMID: 23290512, https://doi.org/10.1016/j.jpeds.2012.11.031.
39. National Asthma Education and Prevention Program. 2007. Expert Panel Report 3 (EPR-3): Guidelines for the Diagnosis and Management of Asthma—Summary Report 2007. J Allergy Clin Immunol 120(suppl 5):S94–S138, PMID: 17983880, https://doi.org/10.1016/j.jaci.2007.09.043.
40. Johansen ME, Reilly CA, Yost GS. 2006. TRPV1 antagonists elevate cell surface populations of receptor protein and exacerbate TRPV1-mediated toxicities in human lung epithelial cells. Toxicol Sci 89(1):278–286, PMID: 16120755, https://doi.org/10.1093/toxsci/kfi292.
41. Fontalba A, Gutierrez O, Fernandez-Luna JL. 2007. NLRP2, an inhibitor of the NF-κB pathway, is transcriptionally activated by NF-κB and exhibits a nonfunctional allelic variant. J Immunol 179(12):8519–8524, PMID: 18056399, https://doi.org/10.4049/jimmunol.179.12.8519.
42. Tilburgs T, Meissner TB, Ferreira LMR, Mulder A, Musunuru K, Ye J, et al. 2017. NLRP2 is a suppressor of NF-κB signaling and HLA-C expression in human trophoblasts. Biol Reprod 96(4):831–842, PMID: 28340094, https://doi.org/10.1093/biolre/iox009.
43. Gao S, Sun Y, Zhang X, Hu L, Liu Y, Chua CY, et al. 2016. IGFBP2 activates the NF-κB pathway to drive epithelial–mesenchymal transition and invasive character in pancreatic ductal adenocarcinoma. Cancer Res 76(22):6543–6554, PMID: 27659045, https://doi.org/10.1158/0008-5472.CAN-16-0438.
44. Ben-Shmuel A, Shvab A, Gavert N, Brabletz T, Ben-Ze'ev A. 2013. Global analysis of L1-transcriptomes identified IGFBP-2 as a target of ezrin and NF-κB

signaling that promotes colon cancer progression. Oncogene 32(27):3220–3230, PMID: 22869145, https://doi.org/10.1038/onc.2012.340.
45. Guo Q, Yu DY, Yang ZF, Liu DY, Cao HQ, Liao XW. 2020. IGFBP2 upregulates ZEB1 expression and promotes hepatocellular carcinoma progression through NF-κB signaling pathway. Dig Liver Dis 52(5):573–581, PMID: 31818638, https://doi.org/10.1016/j.dld.2019.10.008.
46. Zhang BY, Zhang YL, Sun Q, Zhang PA, Wang XX, Xu GY, et al. 2020. Alpha-lipoic acid downregulates TRPV1 receptor via NF-κB and attenuates neuropathic pain in rats with diabetes. CNS Neurosci Ther 26(7):762–772, PMID: 32175676, https://doi.org/10.1111/cns.13303.
47. Schins RP, Donaldson K. 2000. Nuclear factor kappa-B activation by particles and fibers. Inhal Toxicol 12(suppl 3):317–326, PMID: 26368631, https://doi.org/10.1080/08958378.2000.11463241.
48. Simeonova PP, Luster MI. 1996. Asbestos induction of nuclear transcription factors and interleukin 8 gene regulation. Am J Respir Cell Mol Biol 15(6):787–795, PMID: 8969274, https://doi.org/10.1165/ajrcmb.15.6.8969274.
49. Giridharan S, Srinivasan M. 2018. Mechanisms of NF-κB p65 and strategies for therapeutic manipulation. J Inflamm Res 11:407–419, PMID: 30464573, https://doi.org/10.2147/JIR.S140188.
50. Kim SW, Schifano M, Oleksyn D, Jordan CT, Ryan D, Insel R, et al. 2014. Protein kinase C-associated kinase regulates NF-κB activation through inducing IKK activation. Int J Oncol 45(4):1707–1714, PMID: 25096806, https://doi.org/10.3892/ijo.2014.2578.
51. Saha RN, Jana M, Pahan K. 2007. MAPK p38 regulates transcriptional activity of NF-κB in primary human astrocytes via acetylation of p65. J Immunol 179(10):7101–7109, PMID: 17982102, https://doi.org/10.4049/jimmunol.179.10.7101.
52. Refsnes M, Skuland T, Låg M, Schwarze PE, Øvrevik J. 2014. Differential NF-κB and MAPK activation underlies fluoride- and TPA-mediated CXCL8 (IL-8) induction in lung epithelial cells. J Inflamm Res 7:169–185, PMID: 25540590, https://doi.org/10.2147/JIR.S69646.
53. Bhave G, Hu HJ, Glauner KS, Zhu W, Wang H, Brasier DJ, et al. 2003. Protein kinase C phosphorylation sensitizes but does not activate the capsaicin receptor transient receptor potential vanilloid 1 (TRPV1). Proc Natl Acad Sci USA 100(21):12480–12485, PMID: 14523239, https://doi.org/10.1073/pnas.2032100100.
54. Mandadi S, Numazaki M, Tominaga M, Bhat MB, Armati PJ, Roufogalis BD. 2004. Activation of protein kinase C reverses capsaicin-induced calcium-dependent desensitization of TRPV1 ion channels. Cell Calcium 35(5):471–478, PMID: 15003856, https://doi.org/10.1016/j.ceca.2003.11.003.
55. Islam T, Berhane K, McConnell R, Gauderman WJ, Avol E, Peters JM, et al. 2009. Glutathione-S-transferase (GST) P1, *GSTM1*, exercise, ozone and asthma incidence in school children. Thorax 64(3):197–202, PMID: 18988661, https://doi.org/10.1136/thx.2008.099366.
56. Joubert BR, Reif DM, Edwards SW, Leiner KA, Hudgens EE, Egeghy P, et al. 2011. Evaluation of genetic susceptibility to childhood allergy and asthma in an African American urban population. BMC Med Genet 12:25, PMID: 21320344, https://doi.org/10.1186/1471-2350-12-25.
57. Charrad R, Kaabachi W, Rafrafi A, Berraies A, Hamzaoui K, Hamzaoui A. 2017. IL-8 gene variants and expression in childhood asthma. Lung 195(6):749–757, PMID: 28993876, https://doi.org/10.1007/s00408-017-0058-6.
58. Sadeghnejad A, Karmaus W, Arshad SH, Kurukulaaratchy R, Huebner M, Ewart S. 2008. *IL13* gene polymorphisms modify the effect of exposure to tobacco smoke on persistent wheeze and asthma in childhood, a longitudinal study. Respir Res 9(1):2, PMID: 18186920, https://doi.org/10.1186/1465-9921-9-2.
59. Sadeghnejad A, Meyers DA, Bottai M, Sterling DA, Bleecker ER, Ohar JA. 2007. *IL13* promoter polymorphism –1112C/T modulates the adverse effect of tobacco smoking on lung function. Am J Respir Crit Care Med 176(8):748–752, PMID: 17615386, https://doi.org/10.1164/rccm.200704-543OC.
60. Wang Z, Chen C, Niu T, Wu D, Yang J, Wang B, et al. 2001. Association of asthma with β_2-adrenergic receptor gene polymorphism and cigarette smoking. Am J Respir Crit Care Med 163(6):1404–1409, PMID: 11371409, https://doi.org/10.1164/ajrccm.163.6.2001101.
61. Kousha A, Mahdavi Gorabi A, Forouzesh M, Hosseini M, Alexander M, Imani D, et al. 2020. *Interleukin 4* gene polymorphism (–589C/T) and the risk of asthma: a meta-analysis and met-regression based on 55 studies. BMC Immunol 21(1):55, PMID: 33087044, https://doi.org/10.1186/s12865-020-00384-7.
62. CDC (Centers for Disease Control and Prevention). 2022. Most recent national asthma data. Last reviewed 13 December 2022. https://www.cdc.gov/asthma/most_recent_national_asthma_data.htm [accessed 1 July 2022].
63. Luostarinen S, Hämäläinen M, Moilanen E. 2021. Transient receptor potential ankyrin 1 (TRPA1)-an inflammation-induced factor in human HaCaT keratinocytes. Int J Mol Sci 22(7):3322, PMID: 33805042, https://doi.org/10.3390/ijms22073322.
64. Luostarinen S, Hämäläinen M, Hatano N, Muraki K, Moilanen E. 2021. The inflammatory regulation of TRPA1 expression in human A549 lung epithelial cells. Pulm Pharmacol Ther 70:102059, PMID: 34302984, https://doi.org/10.1016/j.pupt.2021.102059.
65. Hatano N, Itoh Y, Suzuki H, Muraki Y, Hayashi H, Onozaki K, et al. 2012. Hypoxia-inducible factor-1α (HIF1α) switches on transient receptor potential ankyrin repeat 1 (*TRPA1*) gene expression via a hypoxia response element-like motif to modulate cytokine release. J Biol Chem 287(38):31962–31972, PMID: 22843691, https://doi.org/10.1074/jbc.M112.361139.
66. Hatano N, Matsubara M, Suzuki H, Muraki Y, Muraki K. 2021. HIF-1α dependent upregulation of ZIP8, ZIP14, and TRPA1 modify intracellular Zn^{2+} accumulation in inflammatory synoviocytes. Int J Mol Sci 22(12):6349, PMID: 34198528, https://doi.org/10.3390/ijms22126349.
67. Huang KP. 1989. The mechanism of protein kinase C activation. Trends Neurosci 12(11):425–432, PMID: 2479143, https://doi.org/10.1016/0166-2236(89)90091-x.